Informes Técnicos Ciemat

805

Diciembre 1996

Pool scrubbing

J. López-Jiménez
L.E. Herranz
M.J. Escudero
M.M. Espigares
V. Peyrés
J. Polo
Ch. Kortz
M.K. Koch
U. Brockmeier
H. Unger
L.M.C. Dutton
Ch. Smedley
W. Trow
A.V. Jones
E. Bonanni
M. Calvo
A. Alonso

Instituto de Tecnología Nuclear

Toda correspondencia en relación con este trabajo debe dirigirse al Servicio de Información y Documentación, Centro de Investigaciones Energéticas, Medioambientales y Tecnológicas, Ciudad Universitaria, 28040-MADRID, ESPAÑA.

Las solicitudes de ejemplares deben dirigirse a este mismo Servicio.

Los descriptores se han seleccionado del Thesauro del DOE para describir las materias que contiene este informe con vistas a su recuperación. La catalogación se ha hecho utilizando el documento DOE/TIC-4602 (Rev. 1) Descriptive Cataloguing On-Line, y la clasificación de acuerdo con el documento DOE/TIC.4584-R7 Subject Categories and Scope publicados por el Office of Scientific and Technical Information del Departamento de Energía de los Estados Unidos.

Depósito Legal: M-14226-1995
NIPO: 238-96-001-0
ISSN: 1135-9420

Editorial CIEMAT

CLASIFICACIÓN DOE Y DESCRIPTORES

220504, 220900
SCRUBBING, HYDRODYNAMICS, SOURCE TERMS, FISSION PRODUCTS, AEROSOLS, EXPERIMENTAL DATA, COMPUTER CODES, BUBBLES, PONDS

"Pool scrubbing"

López-Jiménez, J.; Herranz, L.E.; Escudero, M.J.; Espigares, M.M.; Peyrés, V.; Polo, J.
(CIEMAT, SPAIN). Kortz, Ch..; Koch, M.K.; Brockmeier, U.; Unger, H. (RUB-NES, GERMANY).
Dutton, L.M.C.; Smedley, Ch.; Trow, W. (NNC Limited, ENGLAND).
Jones, A.V.; Bonanni, E. (JRC-Ispra, CEC). Calvo, M.; Alonso, A. (UPM, SPAIN)
50 págs., 10 figrs., 7 refs.

Abstract

The Source Term Project in the Third FrameWork Programme of the European Union was conducted under an important joined effort on pool scrubbing research. CIEMAT was the Task Manager of the project and several other organizations participated in it: JRC-Ispra, NNC Limited, RUB-NES and UPM.

The project was divided into several tasks. A peer review of the models in the pool scrubbing codes SPARC90 and BUSCA-AUG92 was made, considering the different aspects in the hydrodynamic phenomenology, particle retention and fission product vapor absortion. Several dominant risk accident sequences were analyzed with MAAP, SPARC90 and BUSCA-AUG92 codes, and the predictions were compared. A churn-turbulent model was developed for the hydrodynamic behaviour of the pool. Finally, an experimental programme in the PECA facility of CIEMAT was conducted in order to study the decontamination factor under jet injection regime, and the experimental observations were compared with the SPARC and BUSCA codes.

"Retención de aerosoles y productos de fisión en piscinas"

López-Jiménez, J.; Herranz, L.E.; Escudero, M.J.; Espigares, M.M.; Peyrés, V.; Polo, J.
(CIEMAT, SPAIN). Kortz, Ch..; Koch, M.K.; Brockmeier, U.; Unger, H. (RUB-NES, GERMANY).
Dutton, L.M.C.; Smedley, Ch.; Trow, W. (NNC Limited, ENGLAND).
Jones, A.V.; Bonanni, E. (JRC-Ispra, CEC). Calvo, M.; Alonso, A. (UPM, SPAIN)
50 págs., 10 figrs., 7 refs.

Resumen

En el proyecto Término fuente del III Programa Marco de la Unión Europea se llevó a cabo una gran tarea conjunta de investigación y desarrollo en la retención de aerosoles y productos de fisión en volúmenes acuosos. El CIEMAT actuó como coordinador del proyecto, en el que participaron, además del CIEMAT, los siguientes organismos: JRC-Ispra, NNC Limited, RUB-NES y UPM.

El proyecto se dividió en diferentes subtareas. Se realizó una revisión profunda de los modelos implementados en los códigos de piscina SPARC90 y BUSCA-AUG92, considerando los distintos aspectos de la fenomenología hidrodinámica, de retención de partículas y de absorción de vapores de productos de fisión. Se analizaron varias secuencias accidentales dominantes de riesgo y se modelizó la fenomenología de retención con los códigos MAAP, SPARC90 y BUSCA-AUG92, comparando las distintas predicciones de estos. Se desarrolló un modelo para el flujo pistonado en piscinas. Finalmente, se desarrolló un programa experimental en la instalación PECA del CIEMAT para el análisis del factor de descontaminación en régimen de chorro, cuyos resultados fueron comparados con las predicciones de los códigos de piscina.

TABLE OF CONTENTS

LIST OF TABLES

LIST OF FIGURES

LIST OF ACRONYMS

ACE	Advanced Containment Experiments
AMMD	Aerodymanic Mass Median Diameter
BUSCA	Bubble Scrubbing Algorithym
BWR	Boiling Water Reactor
CIEMAT	Centro de Investigaciones Energéticas MedioAmbientales y Tecnológicas
DF	Decontamination Factor
EPRI	Electric Power Research Institute
EPSI	Experimental Facility for Pool Scrubbing Investigation
GE	General Electric
GSD	Geometric Standard Deviation
JAERI	Japan Atomic Energy Research Institute
JRC	Joint Research Centre
LACE	LWR Aerosol Containment Experiment
LOFT	Loss of Fluid Test
LP-FP-2	Low Pressure Fission Product
LWR	Light Water Reactor
MAAP	Modular Accident Analysis Program
MCCI	Molten Core Concrete Interaction
MMD	Mass Median Diameter
ORNL	Oak Ridge National Laboratory
POSEIDON	Pool Scrubbing Effect on Iodine Decontamination
PSI	Paul Scherrer Institute
PWR	Pressurized Water Reactor
RCS	Reactor Coolant System
RHR	Residual Heat Removal System
RUB-NES	Ruhr University Bochum, Department of Nuclear and New Energy Systems
SG	Steam Generator
SGTR	Steam Generator Tube Rupture
SPARC	Suppression Pool Aerosol Removal Code
SUPRA	Suppression Pool Retention Analysis
UKAEA	United Kindom Atomic Energy Authority
UPM	Polytechnical University of Madrid
VMD	Volume Mean Diameter

NOMENCLATURE

a	Major semiaxis of ellipsoid
b	Minor semiaxis of ellipsoid
d_b	Bubble diameter
d_{cr}	Critical globule diameter
d_G	Globule diameter
d_p	Particle diameter
d_I	Injection orifice diameter
m	Mass
m	Mass flow rate
P	Total pressure
Q	Volumetric gas flow rate at the injection
S	Submergence
T	Pool temperature
u_s	Gas superficial velocity
U_b	Bubble rise velocity
X	Molar fraction

κ	Time constant for the retention (retention constant)
Φ	Bubble semiangle

Subindex

atm	atmosphere
exp	experimental
in	inlet
inj	injection
out	outlet
rise	rise

1. INTRODUCTION

Decontamination of particle-bearing bubbles as they pass through pools was considered as a key issue susceptible to be addressed within the Source Term Project of the Third Framework Programme. After carrying out a peer literature survey to update the state of the art on this matter, a joint effort among different organizations was done to improve understanding of such a complex phenomenology. Table I summarizes organizations involved and work distribution.

Table I
Overall Work Programme

Partners	Work Description
CIEMAT (Task Manager)	. Separate effect models and data . Influence of hydrodynamics on retention . Role of submicron particles . Fission product vapour scrubbing . Experimental programme
JRC - Ispra	. Coordination with EPSG
NNC	. Impact of pool scrubbing on Source Term
RUB-NES	. Pool scrubbing in the churn-turbulent regime
UPM	. Pool scrubbing database

As can be seen a quite extensive work programme was addressed. Several topics were covered: impact of pool scrubbing on source term assessments, pool scrubbing under churn-turbulent regime, separate effects linked to pool scrubbing (i.e., hydrodynamics, aerosol retention and fission product vapour absorption), pool scrubbing experimental project, etc.

A work plan was agreed among partners concerning the second phase of the RCA (January 1994 - June 1995). It consisted of two phases. The former, called review and assessment, was aimed at defining a suitable test matrix on pool scrubbing. Among activities performed, it can be mentioned: plant assessments, literature surveys, model comparisons and sensitivity studies. The latter, called enlargement and development, was aimed at performing an experimental plan, based on previous studies, which provided relevant data and allowed code validation under representative conditions. Models review was essentially centred on SPARC-90 [1] and BUSCA-AUG92 [2,3] formulation.

This report is aimed at summarizing the major findings and conclusions drawn from all the activities forming pool scrubbing task. Therefore, a closer examination of specifics concerning each piece of work presented below should be sought in the complementary final reports of each organization, which are referenced along the text and where supporting technical references can be found. The report is structured in two main bodies: Model Assessments and Database Enlargement. The first one outlines the work carried out on model shortcomings and capabilities to predict expected situations in case of a severe accident and

the advances got in new model developments. The second one is mainly devoted to a description of the results obtained in the pool scrubbing tests and the supporting hydrodynamic experimental programme and their interpretation.

2. MODEL ASSESSMENTS

In this chapter several sections are included: plant assessment studies, pool scrubbing under churn-turbulent regime, separate effect and sensitivity studies and current model shortcomings.

2.1. Plant Analyses

Plant assessments were performed by NNC and boundary conditions were provided to CIEMAT to carry out pool scrubbing calculations with SPARC-90 and BUSCA-AUG92 codes under representative conditions of dominant risk severe accident sequences. Scenarios analyzed were those corresponding to SGTR sequence and RHR-bypass sequence . No data were available in MAAP output on particle size of aerosols coming into the pools, so that a lognormal distribution described by an AMMD of 1 μm and a GSD of 1.5 was chosen as a reference case. In addition parametric studies were carried out to know DF sensitivity to particle size and to submergence uncertainties. A further more detailed work description can be found in refs. [4,5].

According to events sequence, the overall pool scrubbing time was discretized in periods. Such time intervals were chosen according to the pattern of gas flows and aerosol mass coming into the pool. Two fundamental assumptions were taken: to restrict the study to cesium iodide (CsI), cesium hydroxide (CsOH) and molybdenum dioxide (MoO_2) and to consider them as particles.

Results were obtained for CsI, CsOH and MoO_2 in terms of interval (DF_i^j) and total DFs (DF_i^T); likewise a global DF (DF^G) was estimated. Compound and total DFs were based on interval ones predictions by:

$$DF^G = \frac{\sum_i m_i^{in}}{\sum_i \frac{m_i^{in}}{DF_i^T}} \qquad (1)$$

$$DF_i^T = \frac{m_i^{in}}{\sum_j \frac{m_{ij}^{in}}{DF_i^j}}$$

i=CsI, CsOH and MoO_2; j refers to time intervals; m^{in} is the incoming mass.

The results obtained are summarized in Table II where base case DFs for MAAP, SPARC and BUSCA are presented.

Table II
MAAP, SPARC and BUSCA DFs in pool scrubbing sequences

	RHR			SGTR		
	MAAP	SPARC	BUSCA	MAAP	SPARC	BUSCA
CsI	3.4	4.7	1.7	4.4	28.5	2.7
CsOH	3.1	3.6	1.5	4.6	42.0	3.0
MoO_2	44.1	58.4	3.2	4.5	2.5	1.14
TOTAL	4.7	5.6	1.9	4.55	9.82	2.24

The main observation is the low values of the total DF predicted by any of these codes. In general, MAAP predictions were in between those of SPARC and BUSCA, except for the case of unsoluble material (MoO_2) under SGTR conditions. BUSCA estimated in all the cases lower DFs than SPARC. However, as can be seen in the table, DFs variations among the three different compounds were qualitatively consistent.

As can be inferred from Eq. 1, total DF is dependant upon the mass of each compound entering the pool and the prevailing pool scrubbing conditions during mass injection. This last factor is one of the keys to understand DF compounds in the table. Unexpectedly, MoO_2 shows a higher DF than CsI and CsOH in RHR sequence. The MoO_2 unsolubility would prevent its growth according to pool scrubbing codes formulation, so that inertial mechanisms would be less efficient than in the case of soluble compound (as CsI and CsOH). However, the result obtained is not inconsistent with this phenomenology, but it is a consequence of the MoO_2 inlet in the pool while pool scrubbing was enhanced by boundary conditions. On the other hand, a substantial amount of CsI and CsOH came into the pool in time intervals in which pool absorption efficiency had become lower.

The most efficient mechanism removing fission products from the gaseous stream to the pool were dependent on code and particle nature. In RHR sequence both codes agreed that most of the mass was retained due to condensation at the entrance of the pool during the first period. In SGTR sequences both codes predictions also coincided as well in that the major removal mechanism was impaction at the entrance of the pool for soluble particles; however, for unsoluble particles BUSCA estimated entrance impaction as the most important mechanism whereas SPARC assigned most of the scrubbing during bubble rise through pool (i.e., inertial mechanisms and sedimentation)

The impact of the Decontamination Factors given in Table II on the source term and the resulting dose to the public has been assessed by comparison with the results of MAAP analyses. MAAP is a code used for Probabilistic Safety Analysis, the pool scrubbing component of which is based on correlations of the results generated by the SUPRA code. For a risk assessment, the predicted releases for all accidents are grouped into Release Categories which are defined principally in terms of the dose to the public, with ranges of a factor of ten between categories, but also in terms of the characteristics of the release, for example, the magnitude and duration.

In the case of the SGTR accident, the major contributors to the dose to the public, evaluated from the MAAP results are caesium (49%), iodine (29%) and ruthenium (19%). The first two elements are predicted to be released from the primary circuit in the form of soluble aerosols and the latter element is released in the form of unsoluble aerosol. Table II shows that the Decontamination factors predicted by the BUSCA code are between approximately 2 to 4 times less than those predicted by MAAP for both soluble and unsoluble species. The associated increase in the release to the environment results in a dose increase of 50% with similar major contributors. These changes are insufficient to affect the release category assignment of this fault as derived from the MAAP results. In the case of the SPARC code, compared to the MAAP results, the predicted Decontamination Factors are up to 10 times higher for soluble species (CsI and CsOH) and approximately a factor of 2 lower for the unsoluble species. Because caesium and iodine are the dominant contributors to the dose, the resulting dose is reduced by 70% which would be sufficient to assign the fault to a less onerous release category.

In the case of the RHR accident, the major contributors to the dose to the public, evaluated from the MAAP results, are caesium (64%) and iodine (29%), both in soluble form. Insoluble species do not contribute significantly to the dose since MAAP predicts a high Decontamination Factor for these species. From Table II, the Decontamination Factors for soluble species predicted by the BUSCA code are again a factor of 2 lower than the MAAP values and more than a factor of 10 lower for unsoluble species. Based on the BUSCA predictions, therefore, the release of soluble species will be slightly larger than predicted by MAAP, and the release of unsoluble species will be significantly larger. The resulting dose to the public is, however, only increased by a factor of 2 with little effect on the dose contributors. These changes are not sufficient to affect the assignment of the accident to a release category. In the case of the SPARC predictions, the Decontamination Factors for both soluble and unsoluble species are slightly higher than predicted by MAAP resulting in a reduction in the dose of approximately 30 % but, again, insufficient to affect the assignment of the accident to a release category.

Table III

SPARC and BUSCA predictions of the DF as a function of the particle size

		CsI		CsOH		MoO_2	
Secuencia	AMMD	SPARC	BUSCA	SPARC	BUSCA	SPARC	BUSCA
RHR	0.1 μm	1.9	1.4	1.5	1.3	51.2	2.5
	1.0 μm	4.6	1.7	3.6	1.5	58.2	3.2
	10 μm	417.2	141.2	348.0	130.7	$5.5\ 10^{3}$	265.0
SGTR	0.1 μm	1.2	1.0	1.2	1.0	1.1	1.3
	1.0 μm	27.3	2.7	42.0	3.0	2.5	1.1
	10 μm	$5.3\ 10^{21}$	$8.8\ 10^{3}$	$1.1\ 10^{26}$	$7\ 10^{4}$	$4.8\ 10^{7}$	288.6

Sensitivity studies were carried out on particle size and submergence. DF sensitivity to particle size was analyzed for both sequences. The AMMD ranged from 10^{-1} to 10 μm and GSD was kept constant (1.5). In Table III the results obtained are presented. It can be noted that the uncertainty associated to particle size could largely influence DF estimations. Nonetheless, it was observed that as condensation of steam onto the bubble surface takes place (RHR), such a dependance is not that strong.

Submergence studies were focused on SGTR sequence. They showed that submergence is not a crucial parameter for DF calculations. This little effect on DF was due to the majoritary retention occurring at the injection point, being removal mechanisms during bubble rise only responsible of a small fraction of the total mass retained. However, an interesting difference in the qualitative behaviour of SPARC and BUSCA can be seen in Table IV. SPARC estimated that DF grows under SGTR conditions as submergence is lowered below a certain value of water height above injector. This behaviour is associated to "quencher mechanisms", included in SPARC but not in BUSCA (see section 2.3.3).

Table IV

SPARC and BUSCA predictions of the DF as a function of the submergence for SGTR

	CsI		CsOH		MoO_2	
Submergence	SPARC	BUSCA	SPARC	BUSCA	SPARC	BUSCA
7.0	27.3	2.7	42.0	3.0	2.5	1.1
4.0	15.7	2.3	21.6	2.4	1.8	1.1
2.5	14.9	2.3	18.9	2.3	1.8	1.1
1.5	17.1	-	20.5	-	2.1	-
0.5	32.3	-	38.2	-	3.3	-

2.2 Pool Scrubbing under Churn-Turbulent Regime

Gas can rise-up through pools under churn-turbulent flow regime. NES at the Ruhr University Bochum was in charge of extending existing models for bubbly flow in codes to the churn turbulent flow fission product scrubbing. The approach followed consisted in extending existing models for bubbly flow to the churn turbulent regime. BUSCA, SPARC and SUPRA retention models rely on boundary conditions largely dependant on hydrodynamics, which provides basic parameters like the gas-liquid exchange surface or the gas residence time in the pool. A further more detailed description will be given in a forthcoming individual final report concerning the RUB/NES activities for pool scrubbing in the churn turbulent flow regime [6].

Emphasis in model development was devoted to the characteristic differences between bubbly and churn turbulent bubble behaviour in liquid pools. As a first step the basic flow patterns in vertical two-phase flows and the transition regimes were analyzed. The two-phase flow behaviour in channels is greatly affected by the vicinity of the confining walls and the movement of the liquid phase. Thus, in case of a gas sparging a large diameter pool containing water at rest, significant differences regarding the governing flow regimes are to be expected.

At low gas flows injected into the pool, uniformly sized bubbles rising in the liquid are observed. This is in analogy to the bubbly flow regime observed in tube flows. However, with increasing gas flow, the slug flow regime expected is not observed in pool geometries. Since the pool is larger in diameter than the maximum stable bubble diameter, the Taylor bubbles -characteristic of slug flow- are unstable. This implies that for experimental investigations concerning the hydrodynamic phenomena in water pool, the pool diameter must be sufficiently larger than the maximum stable Taylor bubble diameter in order to be representative. The annular flow does not occur for the absence of confining walls. With

further increasing gas flow rate, however, pool two-phase flows show a behaviour comparable to the droplet flow regime in tubes.

In case of pool two-phase flows, the transition regime between the bubbly and the droplet flow regime may be denoted as the so-called churn turbulent flow regime. The behavior of the rising bubbles enters into this regime, if the gas flow rate is increased above the values typical for bubbly flow. The transition can be identified for superficial velocities (ratio of volumetric gas flow rate to agitated pool surface area) exceeding 0.1m/s as an order of magnitude. The resulting flow patterns are characterized by the formation of large, irregularly shaped bubbles with high buoyancy. These large bubbles are accompanied by small ones. Regarding the local size distribution, the large bubbles tend to exist more or less in the center of the gas flow, while the small ones are located in the outer regions.

Figure 1 shows qualitatively the flow patterns expected for the two-phase flow in liquid pools as a function of the gas fraction.

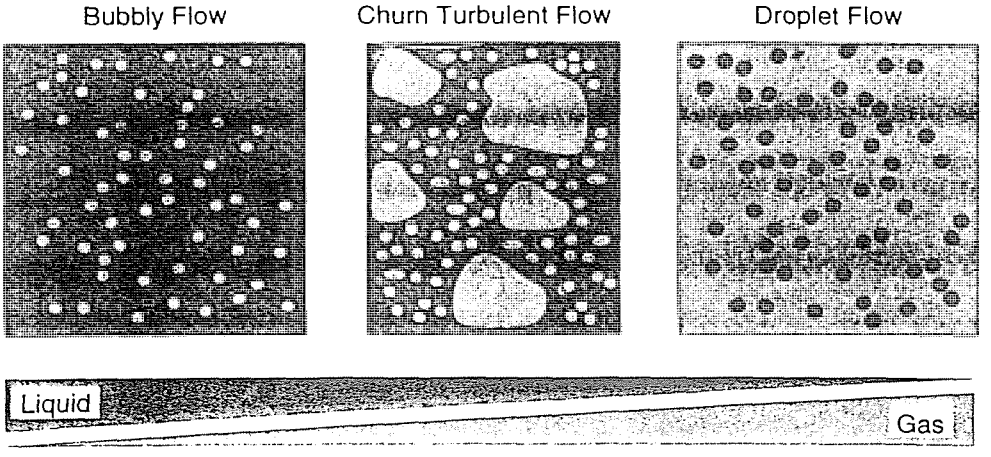

Figure 1. Flow patterns for two-phase flow in a liquid pool

Bubble coalescence marks a governing mechanism initiating the formation of large bubbles, hence affecting the transition from bubbly- to churn turbulent flow regime. In the bubbly flow regime, the uniform sized bubbles rise basically separated from each other. With increasing volumetric gas flow rate, the frequency of bubbles generated at the injection orifice increases and with that the concentration of bubbles in the pool (bubble density). As a result, interactions between single bubbles become more likely and effective. The generation of large bubbles is initiated by the clustering of ellipsoidal bubbles into agglomerations with shapes already tending towards spherical caps. These bubble clusters rise with increased velocity while the individual bubbles coalesce simultaneously after a short period of time. Bubbles in the path of the spherical cap are overtaken and coalesce at its trailing edge.

Basic parameters affecting the formation of large bubbles due to these processes are the flow velocity, the composition of the liquid phase and its physical properties (in particular liquid viscosity).

As a result of the unsteady rise of these large bubbles and their subsequent bursting at the liquid surface, the pool becomes agitated and the liquid interface is highly fluctuating. With

further increasing gas velocity, the amount of gas which is transported through the pool mainly by means of large bubbles increases. At very high gas velocities almost all the gas is transported by means of large bubbles or even clusters of them. This flow pattern is typical for industrial applications of bubble column reactors. In conclusion, the churn turbulent flow regime in water pools can be characterized by:

- Superficial velocities above and order of magnitude of 0.1 m/s
- Agitated, chaotic and unsteady flow patterns
- Large, irregularly shaped bubbles surrounded by a swarm of smaller bubbles
- Coalescence and disintegration of large unstable bubbles

Consequently, with respect to model development, the churn turbulent regime may be interpreted as a flow of parallel rising bubbles with different sizes, different rising velocities and a certain size distribution across the pool. In entering into this regime, the existing bubbly flow models implemented in present codes are expected to fail. The respective transition superficial velocity could clearly be identified.

The basic structure of a model for the description of pool hydrodynamics for churn turbulent gas flow has been designed. It is based on experimental observations of typical portions of the gas flow making their way to the pool surface in form of small bubbles on the one side and large bubbles on the other side. Figure 2 sketches the structure of the churn turbulent model approach by means of a flowchart.

In a first step two macroscopic parameters of the pool hydrodynamics, i.e. the superficial gas velocity and the mean void fraction will be calculated based on the given geometric boundary conditions and the gas flow rate, which is injected into the pool. These are used to identify the transition between bubbly and churn turbulent flow and to trigger the application of the churn turbulent model approach.

Based on the few presently available experimental data on the mean void fraction in the churn turbulent flow regime, a separation of the gas volume in typical portions transported in small and large bubbles is carried out next. Consequently, the hydrodynamic modelling of the churn turbulent flow is carried out for large and small bubbles separately.

A basic parameter for the application of existing aerosol models to the churn turbulent model approach is the gas-liquid interface area. Hence, the determination of size and shape of the bubbles marks the next step in the model. Experimental investigations show that the large irreglarly shaped bubbles behave like the well known spherical cap bubbles rising in swarms of smaller bubbles. In turn, the small bubbles can be described as spherical or ellipsoidal. As a first approach, unless further experimental data are available, the size of the small bubbles can be approximated by the mean bubble diameter observed in bubbly flow experiments. The size of the large bubbles is determined on the basis of the maximum stable bubble diameter.

With the knowledge of size and shape of small and large bubbles and hence, the volume of each bubble as well as the corresponding gas portions transported, the total amount of bubbles in the pool can be calculated. Furthermore, information on the mean gas-liquid exchange surface can be deduced.

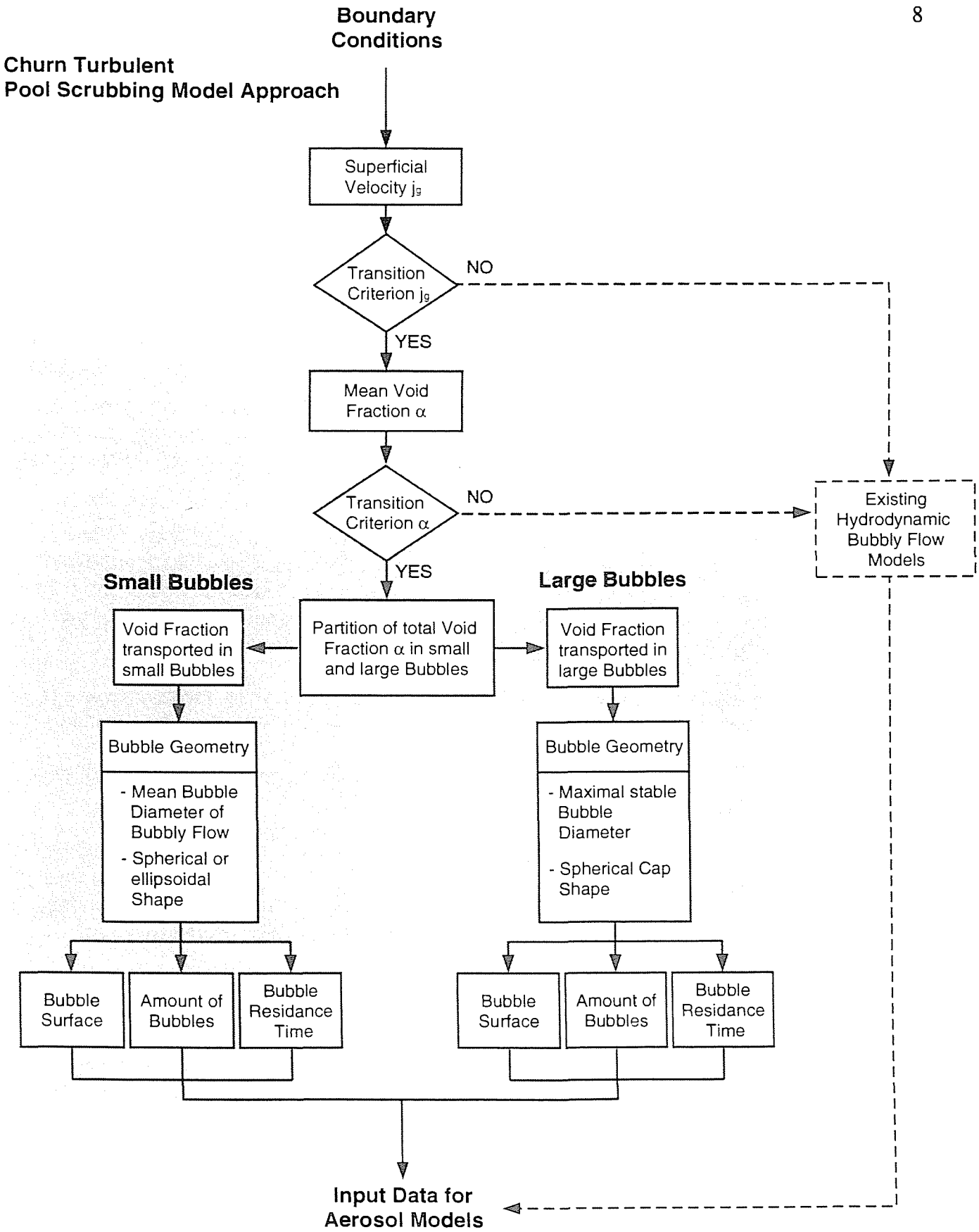

Figure 2. Flowchart of the churn turbulent pool scrubbing model approach

The mean residence time of the bubbles in the pool is given as a function of the injected gas mass flux and the individual gas volumes transported in small and large bubbles in the two-phase mixture. For the small bubble fraction, experimental investigations provide an approximately constant mean rising velocity in the order of magnitude of about 0.2 m/s. The rising velocity of large bubbles changes with the injected gas flux and the void fraction. With the assumption of a approximately constant small bubble rising velocity, the expected large bubble rising velocity can be determined by means of a balance of the transported gas volume fractions in large and small bubbles over the entire pool volume.

Concluding, the required hydrodynamic boundary conditions for the application of already existing aerosol models, i.e., gas-liquid interface area and gas residence time in the pool, are provided by the churn turbulent model approach. For a further development of the churn turbulent model approach, hydrodynamic experimental single effect data obtained under varying gas flow rates in the churn-turbulent flow regime are required. Regarding the pool void fraction, special interest must be taken on the extension of the existing data base concerning the pool void fraction in the churn turbulent flow regime and the corresponding partition of the void fraction in typical portions transported in small and large bubbles. Here, proposals for experimental measurement will be given in the more detailed individual final report. The differences in bubble rise velocity must be analyzed more extensively. Furthermore, the formation and development of large bubbles due to bubble coalescence is under investigation.

Besides pure hydrodynamic data, fission product retention experiments are expected to provide significant data regarding the effective gas-liquid interface, thus allowing for a validation of the gas/liquid interface calculations performed on the basis of hydrodynamic considerations.

2.3 Review of Separate Effect and Sensitivity Studies

According to the Table I topics addressed under this heading were: hydrodynamic effect on aerosol retention, hydrodynamic models, aerosol retention mechanisms and fission product vapour scrubbing. The studies here presented were focused on SPARC-90 and BUSCA-AUG92 codes. More specific information on this work can be found in ref. [5].

2.3.1. Influence of Hydrodynamics on Aerosol Retention

Hydrodynamics is known to be an area of great importance in pool scrubbing. The specific goals of this piece of work were to assess the pool scrubbing database from the hydrodynamic point of view and to identify the most influential hydrodynamic variables in particle absorption during bubble rise. The work was split into two activities: sensitivity studies and literature survey.

A set of parametric studies was performed with SPARC and BUSCA codes to weigh DF sensitivity to variables such as globule diameter and shape, bubble diameter and shape, swarm rise velocity and bubble velocity. The ranges covered of these variables were based on the hydrodynamic models analysis described in next section. The reference scenario chosen was based on LACE-España programme.

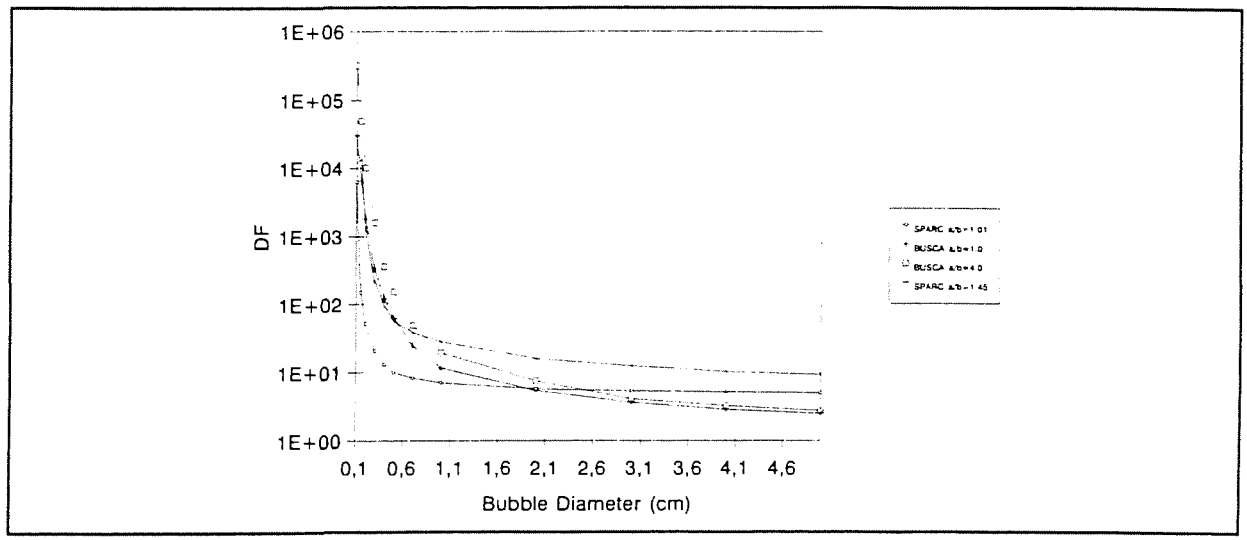

Figure 3. Bubble diameter influence on DF: SPARC and BUSCA results

The hydrodynamic variables seen to be more relevant were the bubble diameter and the swarm rise velocity. In Figures 3 and 4 DF is plotted against bubble diameter and swarm rise velocity, respectively. These two graphs show an exponential shape. Such dependance was expected since both variables are directly involved in the estimation of surface/volume ratio (bubble diameter) and in the residence time (swarm rise velocity), which are factors in DF exponent. The other variables tested did not remarkably affect DF results.

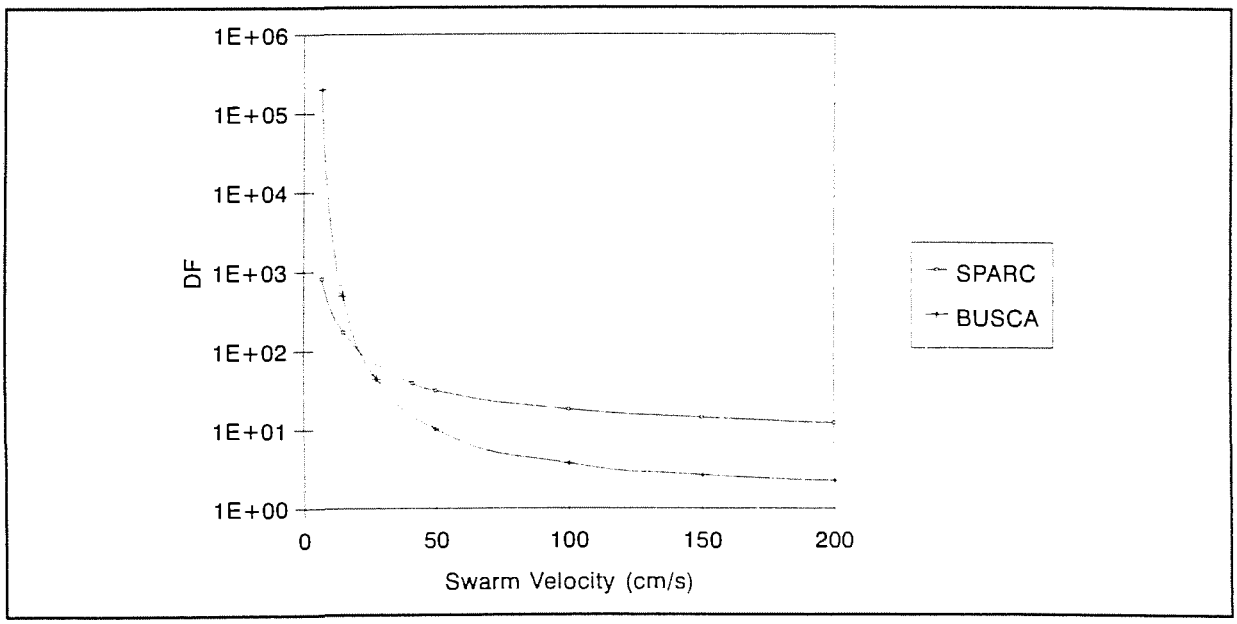

Figure 4. Swarm velocity influence on DF: SPARC and BUSCA results

The results presented above deserve a couple of remarks. First, as gas comes into the pool as a jet, injection zone has a relevant contribution in the total DF. Hence, on one side this high gas velocity regime could suggest other hydrodynamic variables worth to be examined. On the other hand, impacts of bubble diameter and swarm rise velocity would be smoothed.

Second, the primary bubble decay zone could involve variables not accounted for in this study due to model shortcomings which will be commented in next section.

Table V
Pool Scrubbing Experimental Programmes

Programme	Injected Material	Aerosol Size (μm)	Injection Regime	Hydrodynamic Measurements
ACE	CsI, CsOH, MbO	>1	Bubble and Jet	No
EPRI	CsI, TeO_2, Sn	<1	Bubble	Not available
POSEIDON	I_2 vapour		Not available	No
UKAEA	Cr/Ni, I_2 vapour	0.06	Jet	No
LACE-E	CsI	>1	Bubble and Jet	Yes
GE	CsI, EuO_3	$<0.1/0.1$-40	Bubble	Yes
EPSI	CsI	>1	Bubble	No
JAERI	DOP	0.3-10	Bubble	No

A thorough review of available literature on pool scrubbing tests from the hydrodynamic point of view was carried out. It was aimed at finding experimental data confirming at least the theoretical trends observed in SPARC and BUSCA predictions. A total of eight programmes was revised; its major features are summarized in Table V. Once analyzed each individual programme, the major observation was that hydrodynamic measurements were not reported in most of the information written on these tests. An additional difficulty found in tests analysis was the lack of information concerning initial or boundary conditions.

A classification of experiments according to particle nature and size, steam fraction and submergence was done in order to rationalize decontamination factors in terms of hydrodynamic parameters exclusively (Tab. VI). It was readily observed the impossibility of evaluating bubble hydrodynamic effect on DF in most of the experimental programmes revised and of carrying out cross comparisons between those programmes with similar hydrodynamic features because of difference in other relevant parameters such as inlet aerosol size distributions. Nonetheless, based on few data it can be stated that:

- Particle removal is enhanced if gas flows into the pool as a jet rather than in bubble regime.

- Aerosol retention is also increased when using a multiorifice injection device.

Table VI

Hydrodynamic comparison among EPSI, ACE and LACE-España

	S=1 m	S=1.4 m	S=2 m	S=2.5 m	S=2.5 m	S=2.5 m	S=2.5 m	S=2.6 m	S=3 m	S=4.6 m
X_s=1.0	EPSI >3800 4.5 (*) 4.4 --- 0.59 (a) 1.38		EPSI 3700 4.5 (*) 4.4 --- 0.59 (a) 1.38						EPSI 3800 4.5 (*) 4.4 --- 0.59 (a) 1.38	
X_s=0.9				LACE 129/254 3.4 3.38 2.6 0.59 (a) 1.9		LACE 567/922 5.0 3.67 3.8 0.56 (a) 1.79				
X_s=0.6				LACE 419/859 4.2 5.86 3.3 0.64 (a) 1.47		LACE 168/169 3.4 3.69 5.4 0.56 (a) 1.84				ACEA4 1300 2.8 6.12 2.3 0.67 (c) 1.43
X_s=0.4				LACE 677 7.2 3.55 1.6 0.71 (a) 1.61		LACE 16/20 3.4 3.31 1.6 0.72 (a) 1.81				ACE A2 1500 1.7 5.62 2.0 0.70 (c) 1.45
X_s=0.18-0.15				LACE 52/53 5.8 3.38 3.5 0.69 (a) 1.45						
X_s=0.1				LACE 444/702 3.0 3.80 2.3 0.55 (a) 1.99	LACE1273/2913 4.1 4.22 1.8 0.70 (c) 1.45	LACE 491/526 5.6 6.47 3.6 0.71 (b) 1.45	LACE 116/128 1.7 6.53 2.2 0.71 (b) 1.45			
X_s=0.01		ACE A1 47 2.6 6.54 1.9 0.72 (c) 1.46						ACE A3 220 2.7 6.42 2.0 0.72 (c) 1.46		

(*) MMR (Mass Median Radius) (a) Bubbly (b) Jet (c) Multihole

PROGRAMME	DF
AMMD	d_G
	d_b
GSD	a/b

2.3.2. Hydrodynamic Models

Hydrodynamic phenomena governing gas-liquid mixture behaviour is simulated in both SPARC and BUSCA. A peer review of all these models was undertaken to point out the most significant differences between SPARC and BUSCA formulation, as well as their experimental and/or theoretical basis. Particular importance was given to applicability ranges.

In addition to the literature survey, SPARC and BUSCA models were compared numerically. This comparison was done by using a stand-alone code encapsulating all the correlations in SPARC and BUSCA codes. A reference scenario characterized by a subcooled pool (80°C at 1.2 bar) with a injector (1 cm) submergence of 2.0 m in which ga· flows were 0.5 steam fraction and ranged from 1 to 10^5 cc/s was defined. The following models were examined: globule diameter, globule break-up phenomenon, swarm regime, bubble diameter and shape and bubble rise velocity. As a general statement, it can be said that SPARC formulation is mainly based on the pool scrubbing tests carried out by EPRI and GE. Unlike this, BUSCA includes additional correlations and models derived for different scenarios.

There exist several correlations to predict initial globule diameter for different injector configurations in both SPARC and BUSCA. They have been experimentally tested over a wide range of conditions. However, jet flows expected in accident sequences could require an extension of the validation interval covered so far.

Break-up globule phenomenology has been poorly characterized up to now. SPARC and BUSCA approaches are dramatically different. SPARC assumes that the globule size linearly decreases up to disappearing at a distance from the injector about 12 times its initial diameter. In BUSCA, however, the globule disappears instantaneously if two conditions are fulfilled: its size is out of the stability range and it is closer to the injector than ten times its initial diameter.

BUSCA has two stability criteria to define the stability range. However, a look into their formulations and the way they are implemented in the code indicates that the so called Weber criterion is always more restrictive than the Levich one, so that the last one is never used. Next ratio between the maximum diameter allowed in both criteria illustrates this statement:

$$\frac{d_{cr}(Weber)}{d_{cr}(Levich)} = 2.165 \left(\frac{\rho_g}{\rho_l}\right)^{1/3} < 1 \qquad (2)$$

Discrepancies found concerning primary bubble decay approach were seen to be of a certain relevance. In sequences where pool submergence was low and a stable size distribution had not been reached by bubbles rising through the pool, most of gas decontamination occurred in this zone.

Regarding swarm rise velocity, SPARC and BUSCA approaches are also quite different. Whereas BUSCA accounts for different formulations depending upon the grouping of bubbles as clusters or swarms (this is closely related to vent types), SPARC does not consider such a dependence and it defines an only swarm rise velocity. Given the implication of this variable in the estimate of the bubble residence time, this discrepancy could be responsible of quantitative SPARC-BUSCA DF differences.

Bubble diameter and shape formulations are crucial parameters in particle absorption and show outstanding discrepancies between SPARC and BUSCA correlations. SPARC correlates bubble size with noncondensible fraction of the gas flowing into the pool, so that a constant value is held during bubble rise regardless thermohydraulic pool conditions (Fig. 5). However, in BUSCA once globule break-up occurs and an initial diameter is adopted (0.716 cm), it varies along the pool depending on condensation/evaporation process on bubble surface as it rises through the pool (Fig. 6).

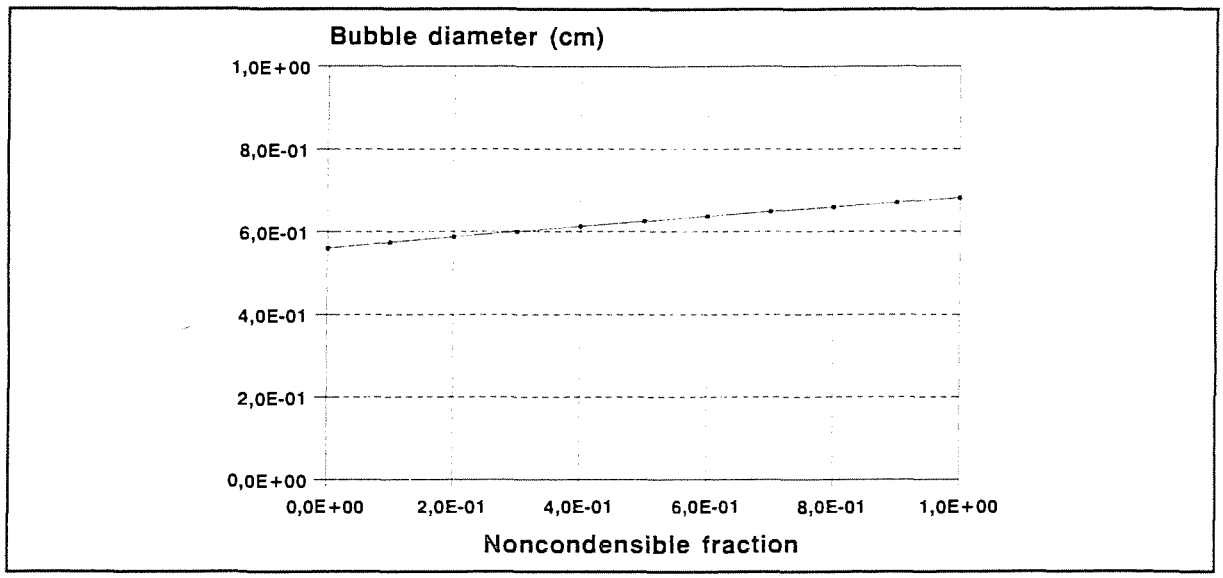

Figure 5. Bubble diameter as a function of noncondensible gas: SPARC formulation

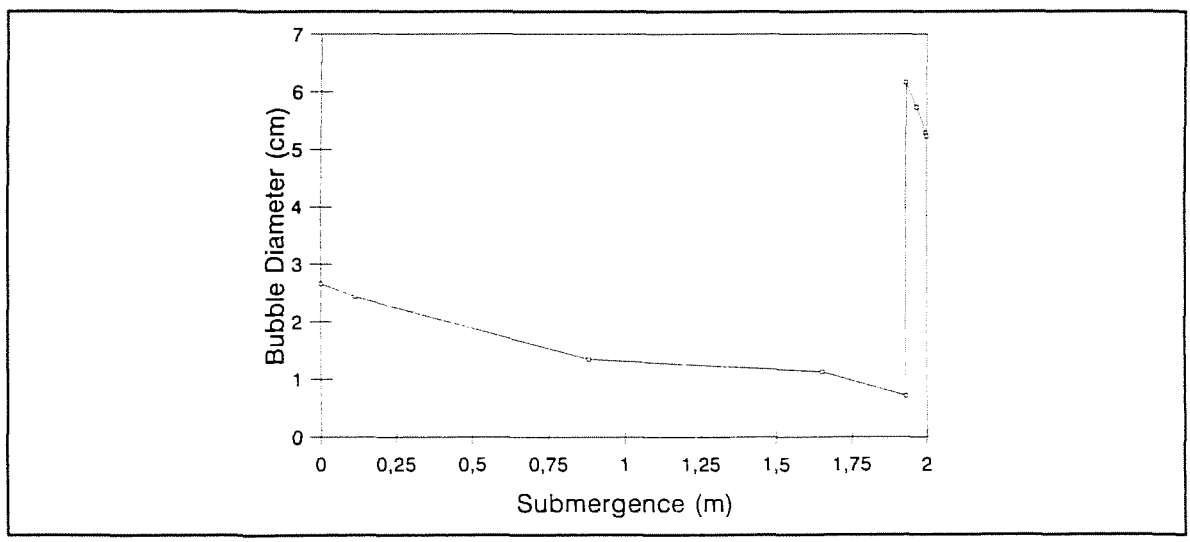

Figure 6. Bubble diameter as a function of submergence: BUSCA formulation (P=1.2 atm, T=372.5 K, inlet gas=N_2)

As said above, bubble shape is modelled quite differently. SPARC considers that bubbles are elliptical and calculates the major to minor axis (a/b) as a function of bubble diameter. BUSCA admits several bubble shapes (spherical, elliptical and caps) and correlates a/b ratio with Eötvos adimensional number. The range of a/b ratio is between 1 and 1.47 for SPARC and between 1. and 4. in the case of BUSCA. Despite this substantial difference, retention

mechanisms in each code do not use a/b ratio the same way, so that a large a/b ratio in BUSCA can have hardly effect on DF, whereas a small a/b ratio in SPARC can affect significantly its predictions.

SPARC and BUSCA have correlations for bubble velocity based on experiments performed in bubbly regime. In spite of discrepancies found (tipically a factor of 2 for bubbles of diameters between 0.5 and 1.0 cm), the major point is on the uncertainty on the rising gas flow regime. As said in section 3, bubbly regime could not be representative of accident scenarios but a more chaotic and fast flow: Churn-Turbulent regime.

2.3.3. Aerosol Retention Mechanisms

Airborne particles within bubbles rising up an aqueous volume undergo physical processes which make a fraction of them be absorbed by the liquid phase. SPARC and BUSCA retention models were compared and calculations to quantitatively weigh the main differences found were carried out.

Particle retention phenomena were grouped in two bins: injection mechanisms and rising bubble mechanisms. This way the DF could be expressed as a product of two factors:

$$DF = DF_{inj} DF_{rise} \qquad (3)$$

Rise-up mechanisms are basically the same in both codes: sedimentation, centrifugal deposition, diffusion, etc. Injection mechanisms were seen to be code-dependant, showing differences in both approaches and phenomena considered.

In Tables VII and VIII the calculation matrix used for the injection sensitivity analysis and the results are presented, respectively. The rest of scenario characteristics can be found in ref. [5].

Table VII
Calculation matrix for the injection sensitivity analysis

Case	Flow (cc/s)	Solubility	AMMD (μm)	T (°C)	X_s
T1	400	Insoluble	1.0	298.2	0.9
C1	400	Insoluble	0.1 1.0 5.0 10.0	353.2	0.1
C2	3000	Insoluble	0.1 1.0 5.0 10.0	353.2	0.1
C3	400	Soluble	0.1 1.0 5.0 10.0	353.2	0.1

Table VIII
Injection sensitivity analysis results

Case	AMMD (μm)	SPARC Impactation	BUSCA Impactation		SPARC Condensation	BUSCA Cond + Term	SPARC Quencher
			SPARC	SUPRA			
T1	1.0	1.00	1.00	1.00	29.60	2.39	1.00
C1	0.1	1.00	1.00	1.00	1.00	1.00	1.01
	1.0	1.00	1.00	1.00	1.00	1.00	1.02
	5.0	1.01	1.02	1.07	1.00	1.00	1.28
	10.0	1.23	1.36	2.27	1.00	1.00	1.96
C2	0.1	1.00	1.00	1.00	1.00	1.00	1.01
	1.0	1.00	1.00	1.00	1.00	1.00	1.11
	5.0	1.68	2.01	6.32	1.00	1.00	2.72
	10.0	8.67	13.01	44.86	1.00	1.00	5.98
C3	0.1	1.00	1.00	1.00	1.00	1.00	1.00
	1.0	1.00	1.00	1.00	1.00	1.00	1.03
	5.0	3.37	1.02	1.07	1.00	1.00	1.28
	10.0	33.10	1.36	2.27	1.00	1.00	1.94

Approximation of particle depletion by steam condensation onto bubble surfaces at the pool inlet is largely different. SPARC assumption of an instantaneous gas-liquid thermal equilibrium removes, if condensing conditions exist, a fraction of particles proportional to the volume of steam condensed. On the contrary, BUSCA calculates the gas-liquid evolution to the equilibrium and, consequently, formulates a removal rate by condensation (i.e., diffusiophoresis and Stefan flow) and by thermophoresis that are effective till gas-liquid equilibrium is reached. The calculations carried out to weigh removal efficiency of steam movement to bubble interface, showed that SPARC largely overpredicts it respect to BUSCA results.

Impaction approach is basically the same in both codes. BUSCA has two different formulations: one is equal to that of SPARC and is exclusively dependant on Stokes adimensional number; the other, taken from SUPRA code, takes also into account bubble and injector dimensions. Calculations performed varying inlet gas flow rates showed that SUPRA model predictions are higher than SPARC ones. However, SPARC estimate of particle growth before impaction makes SPARC results to be the highest in case of soluble aerosols.

Additional contributions at the injection are considered in SPARC if the gas comes into the pool through small orifices: settling, centrifugal deposition and diffusion are modelled while globule is setting up and, eventually, detaches. BUSCA does not simulate these phenomena. SPARC models each mechanism mentioned in a different way depending on the stage of the process: globule expansion or detachment. The analyses performed revealed that centrifugal deposition during globule expansion was the most efficient depletion mechanism.

Particle absorption shows a minimum as a function of particle size during bubble rise up. In this work location of this minimum was shown to be different in SPARC and BUSCA by plotting removal constant of each mechanism and the total one versus particle diameter

(Figure 7). The phenomena considered in this study were: diffusion, settling and centrifugal deposition. This work was carried out with a stand-alone code based on SPARC and BUSCA equations which read bubble and pool conditions from the input deck.

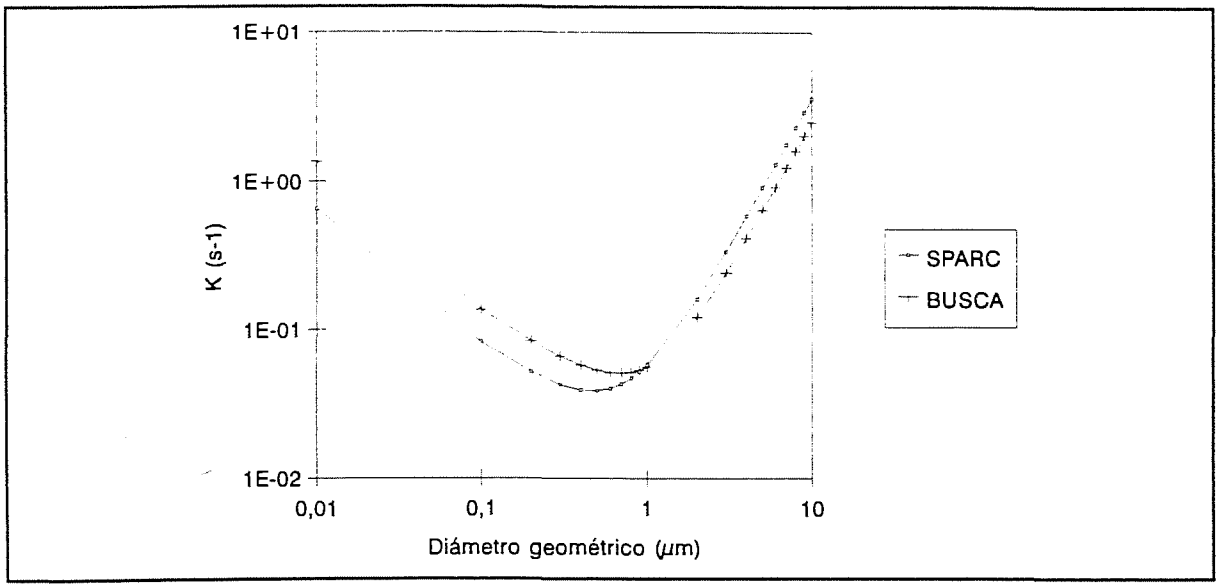

Figure 7. Removal rate constant as a function of particle diameter

Diffusion governs small particle removal. The range of such predominance was seen to be a function of boundary conditions, particularly bubble shape. Despite being both based on the penetration theory, the way of assessing parameters in diffusion velocity equations yields higher velocities in BUSCA than SPARC. Namely, BUSCA code seems to be more efficient removing small particles than SPARC.

Centrifugal deposition was seen to be the dominant removal process followed by sedimentation at particle sizes above approximately 1 μm. Nonetheless, under specific conditions inertial mechanisms predominance can even extend over a significant interval in the submicron range. In this regard formulation discrepancies between SPARC and BUSCA became quite outstanding as bubbles depart from a spherical shape and adopt an ellipsoidal one.

BUSCA approach of centrifugal deposition is based on spherical bubbles, whereas SPARC one accounts for ellipsoidal ones. This different approach results in substantial differences in variables appearing in the equation for non spherical bubbles. On one side, the curvature radius is assumed to be the volume equivalent radius in BUSCA. The higher the bubble eccentricity, the less the accuracy of this approximation. In addition, the angular part of the superficial gas velocity is different. In simple terms, superficial gas velocity can be written in the case of SPARC as,

$$u_s = U_b f(\varphi, a, b) \qquad (4)$$

whereas for BUSCA it is independent of a and b and keeps the same functionality with ϕ regardless bubble geometry:

$$u_s = 1.5\,U_b \sin\varphi \qquad (5)$$

Studies carried out showed that BUSCA assumption on curvature radius was mostly responsible of the quantitative differences found in velocity assessments.

Particular attention was given to submicron particles. Experimental observations pointed out that small particles ($d < 1\mu m$) were hardly retained in pools. However, this statement is subjected to those specific boundary conditions. Retention mechanisms weakly dependant on particle size, such as diffusiophoresis or thermophoresis, are efficient at removing submicron particles. Likewise, as seen in the above figure, diffusion is the dominant retention mechanism for small particles during bubble rise and its removal rate constant can reach significant values. In addition, injection flows expected during accident sequences can be high enough to cause particle depletion at the entrance of the pool by inertial mechanisms. Hence, submicron particle retention is closely linked to prevailing conditions during pool scrubbing, so that it should not be considered negligible a priori. Calculations performed with SPARC and BUSCA under sequence boundary conditions showed a significant fraction of submicron particles retained in the pool.

Even though not a retention mechanism, the soluble particles growth models were analyzed. Despite being based on the Mason Equation, there are significant discrepancies both in the estimate of variables appearing in the growth rate equation and in their numerical treatment ("fixed grid" in SPARC and "moving grid" in BUSCA). To these differences one should add the different way both codes perform their steam balance in the bubble, which strongly influence the estimate of the bulk saturation ratio. A sensitivity study with temperature was carried out. In Table IX the initial size distribution of particles can be seen along with the final ones at the exit of the pool as predicted by SPARC and BUSCA.

Table IX

Inlet and outlet size distribution parameters for the growth sensitivity analysis

	AMMD (μm)	GSD
Inlet	2.5	1.5
SPARC-372.5 K	16.37	1.1
SPARC-298.2 K	3.67	1.5
BUSCA-372.5 K	16.63	1.5
BUSCA-298.2 K	13.78	1.5

It can be seen that both models showed a rather different sensitivity to pool temperature. However, the large amount of possible sources of discrepancies prevented to discern which was the most relevant factor.

2.3.4. Fission Product Vapour Scrubbing

A fraction of fission product inventory can reach pools during hypothetical accidents as vapours. Owing to its radiological impact, particular attention has been given in this regard to iodine. A comparison of SPARC and BUSCA models concerning gaseous iodine absorption by pools was done. This work consisted of: a review of available database, a

study of models implemented in SPARC and BUSCA and their fundamentals, a sensitivity analysis and, finally, an evaluation exercise against experimental data.

There exists experimental information on iodine vapour retention in pools. In the Table X, the experimental programmes carried out along with their main features are presented. Influence of several variables on gaseous iodine retention was looked into. As observed in particle retention, small injection orifices, large steam fractions in the incoming gas and large water above injectors enhance gaseous iodine decontamination. From the chemical point of view, the more influential variables were: the iodine chemical form and its concentration, the pool temperature and the presence of chemicals in the aqueous bulk. The higher the species volatility the lower the partition coefficient and, then, the higher the resistance to be absorbed by pools. The higher the iodine concentration, the lower the gas decontamination. Certain chemicals were seen to enhance aqueous chemical reactions, causing a decrease in system volatility and, hence, a more efficient iodine retention. Temperature influence was observed to be rather complex; it affects diffusion processes, species partition and aqueous chemistry.

Concerning SPARC and BUSCA models several differences were found. SPARC simulates molecular iodine (I_2) and methyl iodide (CH_3I) behaviour. On the contrary, BUSCA model is restricted to I_2. As for the treatment of I_2, even though both codes are based on the penetration theory, approximations taken to derive the final equations implemented in the code are not the same. On one side, BUSCA accounts for the curvature of the bubble and distinguishes a plane and a curved surface. SPARC, however, considers curvature effects only indirectly through the diffusion time estimate. On the other side, BUSCA assumes a null iodine concentration in the aqueous bulk, whereas SPARC calculates an equilibrium distribution of iodine species, fundamentally based on hydrolysis reactions (only for I_2).

Table X

Experimental programmes on fission product vapours retention in pools

Organization	Author	Injected gas	Injector	Submergence (cm) Temperature (C)
PSI (POSEIDON)	S. Güntay	N_2 Injection rate not available	Vertical d_i: 0.5-9 mm	100-400 T : 21, 40, 60
UKAEA	J.J. Hillary et al.	Steam (kg/s) : 0-3.992 Air (kg/s): 0-3.311	Vertical d_i: 10 cm	61 and 30.5 T: 10
UKAEA	H.R.Diffey et al.	% Air/Steam: 0.01-0.1	Vertical d_i:3 y 50 mm	0.6 y 5 T: 28 and 50
ORNL	L.E.Standford C.C. Webster	% Air : 0 y 2 Steam (kg/s): 0.025-0.075	Vertical d_i: 1.72 cm	122 T: 10 - 38
ORNL (GE)	D.P. Siegwarth M. Siegler	Air-Steam	Vertical	30.5- 122 T: 32.2 - 66.6

All the discrepancies presented above were numerically weighed by a set of parametric calculations based on LACE-España as a reference sceanario. Iodine species, temperature,

gas composition and iodine concentration were varied. Their results are summarized in Tables XI and XII.

Table XI
SPARC results for the iodine sensitivity analysis

Case	Injected Gas	Species	T (°C)	Concentration (M)	DF
I1	Air		100	10^{-4}	32.86
I2	"		100	10^{-6}	56796.00
I3	"		25	10^{-4}	550.93
I4	"	I_2	25	10^{-6}	3800.00
I5	Air/steam		100	10^{-4}	117.63
I6	"		100	10^{-6}	194150.00
I7	"		25	10^{-4}	1275.70
I8	"		25	10^{-6}	8803.10
OI1	Air		100	10^{-6}	1.39
OI2	"	CH_3I	25	"	4.05
OI3	Air/steam		100	"	1.67
OI4	"		25	"	6.25

Table XII
BUSCA results for the iodine sensitivity analysis

Case	Injected Gas	Species	T (°C)	Concentration(M)	DF
I1	Air		100	10^{-4}	3371
I2	"		100	10^{-6}	3369
I3	"		25	10^{-4}	12970
I4	"	I_2	25	10^{-6}	12880
I5	Air/steam		100	10^{-4}	10540
I6	"		100	10^{-6}	10720
I7	"		25	10^{-4}	37600
I8	"		25	10^{-6}	39630

SPARC and BUSCA results showed large discrepancies. Unlike SPARC´, BUSCA predictions are not dependant upon the final iodine concentration. In addition, except for low concentration and high temperature cases, BUSCA generally overpredicted the decontamination factor respect to SPARC estimations. The source of these discrepancies seemed to be the different bubble geometry considered and the way the interfacial gaseous side concentration is estimated.

In addition to the sensitivity studies, SPARC and BUSCA models were checked against experimental data. Table XIII shows the calculation matrix used to evaluate models. It is based on UKAEA (Diffey) experiments.

Table XIII

Calculation matrix for the assessment of fission product vapour models

SMALL SCALE FACILITY (Injection time: 30 minutes)				
Species	I_2		CH_3I	
% w air/steam	1	10	1	10
Iodine concentration (M)	Low $4.0\ 10^{-8}$ - $1.6\ 10^{-6}$	High $2.5\ 10^{-6}$ - $1.6\ 10^{-4}$	$5.0\ 10^{-9}$ - $4.0\ 10^{-6}$	
LARGE SCALE FACILITY (Injection time: 60 minutes)				
Species	I_2			
% w air /steam	1		10	
Iodine concentration (M)	Low $4.0\ 10^{-8}$ - $1.6\ 10^{-6}$		High. $2.5\ 10^{-6}$ - $1.6\ 10^{-4}$	

Table XIV

SPARC and BUSCA results versus experimental measurements

Case	Specie	% air/steam	$[I_2]$ (M)	T (°C)	SPARC DF	BUSCA DF	DF_{Exp}
IA1	I_2	1	$4.0\ 10^{-8}$ $1.6\ 10^{-6}$	28	516.4 375.6	- -	2120
IA2	I_2	10	$4.0\ 10^{-8}$ $1.6\ 10^{-6}$	28	53.3 39.0	- -	232
IA3	I_2	1	$2.5\ 10^{-6}$ $1.6\ 10^{-4}$	28	351.7 277.0	- -	390
IA4	I_2	10	$2.5\ 10^{-6}$ $1.6\ 10^{-4}$	28	36.5 28.8	- -	29
IA5	CH_3I	1	$5.0\ 10^{-9}$ $4.0\ 10^{-6}$	28	1.07 1.07	- -	3.72
IA6	CH_3I	10	$5.0\ 10^{-9}$ $4.0\ 10^{-6}$	28	1.067 1.067	- -	1.59
IA7	I_2	10	$4.0\ 10^{-8}$ $1.6\ 10^{-6}$	50	3691.8 35.6	729.6 731.0	908/1695
IA8	I_2	10	$2.5\ 10^{-6}$ $1.6\ 10^{-4}$	50	18.2 2.7	731.1 786.9	1[illegible]

The results obtained with SPARC and BUSCA can be seen in Table VI. SPARC results presented the same trends as experiments: pool absorption efficiency increases at low iodine concentrations and low air fraction in inlet gas. Unlike this, BUSCA did not show any sensitivity to iodine concentration due to the above mentioned model assumption.

2.4. Model shortcomings

Risk dominant sequences analyses along with the sensitivity and evaluation studies came out with several model shortcomings which were seen as relevant concerning pool scrubbing codes capabilities to simulate expected accident scenarios. These shortcomings could be grouped into two bins: model approach and lack of models. Next, a short description of them is given.

2.4.1. Model Approach

Model shortcomings were found in the three areas analyzed: hydrodynamics, particle removal and gaseous iodine absorption.

Most of hydrodynamic formulation encapsulated in pool scrubbing codes are correlations. That is, they should be applied exclusively within the experimental conditions range in which they were developed. None of the existing correlations simulating the gas injection into a pool wholly cover the injection regimes estimated for pool scrubbing sequences. Particularly, an expression describing jet injection regime at very high We numbers should be found and implemented in pool scrubbing codes. This suggests the need of obtaining experimental data to support the theoretical work on this point.

SPARC thermohydraulic assumption of instantaneous gas-pool equilibrium should be carefully studied and validated. Such an assumption has several implications in pool scrubbing: an early decontamination due to steam condensation on bubble surfaces (if condensing conditions prevail); a growth of soluble particles, making them more efficiently retained by inertial mechanisms; a small change of bubbles size as it rises through pools, etc. This approach along with an arbitrary factor of 3 appearing in its formulation should be further checked.

BUSCA formulation of the centrifugal deposition assumed spherical bubbles (applicable to spherical caps as well). Most of the bubbles within the size range of interest in pool scrubbing shows shapes other than the spherical one. Therefore, an extension of this equation to other shapes should be implemented. On the other hand, SPARC formulation is valid for spherical and elliptical bubbles, but it is not applicable to cap shaped bubbles. In addition to this, bubble surface is not regular and oscillates as the bubble rises up in the pool. Both oscillations and small circularities surfaces (i.e., perimeter/area) should be as well accounted for in the equation predicting centrifugal deposition. The importance of this point relies on the fact that removal by centrifugal forces is the major retention mechanism during rise-up of particles bigger than about 1 μm of diameter.

Entrainment phenomenon at pool surface was initially disregarded in pool scrubbing formulation. However, a deeper analysis encompassing both BWR and PWR should be carried out to check its potential effect in all risk-dominant scenarios.

SPARC and BUSCA approaches to I_2 absorption cannot simulate iodine stripping from pools. This situation should be expected whenever an iodine free gas passes through a pool previously contaminated with any iodine species. BUSCA assumption of a null iodine concentration in aqueous bulk prevents to can reproduce such scenarios. SPARC capability is a bit improved. Even though it accounts for iodine chemistry in the pool, it is restricted to hydrolysis related reactions and no consideration of radiolytic processes is done. Besides, pH evolution is very poorly characterized so that pH could not be predicted in real scenarios. In general, the situation seems to be too complex to be coped with by pool scrubbing codes. Coupling of iodine chemistry and pool scrubbing codes could be an acceptable via to account for all this interrelated phenomenology and would also allow to consider other iodine species than I_2, such as organic iodides.

2.4.2. Lack of Models

There are experimental and theoretical evidences of some pool scrubbing related phenomena still not included in codes. Next, some of the most important ones are presented. It should be underlined that all of them would enhance current accident analysis capabilities and would require specific experimental data supporting model development.

Bubbles regime while rising up in the pool is uncertain. Current models assume that bubbly flow is a suitable description. However, as gas flows passing through pools can reach high velocities churn-turbulent could turn into a better way to reproduce bubbles movement. The development and implementation of a churn-turbulent flow for gases crossing large liquid volumes would remarkably affect both hydrodynamics and fission product absorption.

Pool scrubbing can occur in aqueous volumes where surfaces are immersed. In SGTR sequence, for example, thousands of tubes disrupt the aqueous medium continuity. This would imply gas bubbles interactions with surfaces and, thus, their hydrodynamic characterization would be altered. These phenomena, generally called "wall effect", are seen crucial due to their importance in the above quoted risk-dominant sequence.

Hydrodynamics importance on pool scrubbing is beyond question. Accident scenarios are known to be "dirty". Namely, a huge amount of materials would contaminate pools and perturb their properties. Particularly relevant are surfactants whose repercussion on hydrodynamics is known and can significantly affect fission product absorption by pools.

As gas flows into a pool through small orifices, primary bubble formation and detachment from the injector requires a time lag. During such a time, the gas circulates inside the bubble and particles retention by diffusion, settling and centrifugal forces could happen. These processes are approximately accounted for in SPARC but not in BUSCA. Studies should be carried out to ensure the importance of this effect. If confirmed, a check of SPARC model should be done to include it or an alternative formulation in BUSCA.

3. DATABASE ENLARGEMENT

An experimental programme was carried out by CIEMAT in the PECA facility. Much of it was supported by the previous studies presented in the preceding section. Performance of these experiments required facility and protocol modifications from earlier experimental programmes, as well as the use of new aerosol generation techniques. A precise description of the new arrangement of PECA and the test protocol can be found in ref. [7].

3.1. Experimental Programme Definition

The RCA experimental programme consisted of two parts: retention experiments and separate effect tests on hydrodynamics. Both aspects are described below.

3.1.1. Objectives

The interest of the jet injection regime relies on its prediction in analysis performed with different codes (i.e., MAAP, STCP or MELCOR) on risk-dominant accident sequences (i.e., SGTR, RHR, TMLB´ and some BWR sequences). This fact along with the absence or inaccuracy of models simulating expected phenomena turned this area into a crucial point to be addressed by an experimental plan.

The general objective was to enlarge existing database on pool scrubbing under severe accident conditions. The specific objectives were:

- To extend existing database on aerosol retention in pools under jet injection regime.
- To get experimental results on primary bubble formation and upwards movement under prototypical severe accident conditions.
- To correlate pool absorption efficiency measurements and hydrodynamic behaviour.

3.1.2. Pool Scrubbing Tests

A total of four retention tests were carried out. These tests were 30 minutes long. Tests specifications can be seen in Table XV. As can be seen in the table, all parameters were kept constant but submergence. This strategy allowed to look into the effect of submergence on DF as gas comes into the pool under jet regime and to avoid effects overlapping which could prevent a full understanding of the simulated scenario. The scope of this experimental programme suggests that further research on this topic is required at different conditions. Particularly, higher gas flow rates should be tested.

Table XV
Pool scrubbing test matrix

	Injection Conditions		Inlet Gas		Aerosol			Pool Conditions		
	T (C)	P (bar)	Q (cc/s)	X_s	Sp	AMMD (μm)	GSD	T (C)	P_{atm} (bar)	S (m)
RCA1	120	2.8	3000	0.	Ni	3.0	1.4	120	2.3	0.25
RCA2	120	2.8	3000	0.	Ni	3.0	1.4	120	2.3	0.50
RCA3	120	2.8	3000	0.	Ni	3.0	1.4	120	2.3	1.25
RCA4	120	2.8	3000	0.	Ni	3.0	1.4	120	2.3	2.50

Most of conditions in the table came from a compromise between representativeness and test simplicity. Pool conditions were near saturation. Injection and pool conditions were approximated as much as possible to avoid sharp themalhydraulic changes of the carrier gas at the injection and during bubbles rise up. The inlet gas was N_2; it was injected at a volumetric flow rate of 3000 cm^3/s through a 1 cm-diameter hole horizontally oriented. These conditions allowed to reach We numbers ore than a factor of 2 above the onset of jet regime ($We \geq 10^5$). An unsoluble aerosol, metallic Nickel, characterized by an AMMD and a GSD of about 3 μm and 1.4, respectively, was chosen. The only condition required to the aerosol input rate was to be steadfastness during each test.

This set of conditions was supported by preliminary studies with SPARC and BUSCA. Their goal was twofold: to make a good choice of key parameters as inlet gas flow rate and submergence and to obtain DF uncertainty domains as a function of possible variations in particle size characterization. The combination of inlet gas flow rate and submergences seen above was observed o provide enough DF margins to clearly state trends among the experiments. In Figure 8 DF SPARC predictions versus MMD for several GSD values can be seen for 0.5 and 2.5 m submergences. This figure provides DF maps showing dramatic DF changes. This underlined the importance of getting a constant particle size distribution during each test to prevent DF shifts along the time and of reproducing particle size distribution in all the tests since if not a DFs overlapping could mask actual trends. BUSCA calculations did not show remarkable variations, being their higher predictions around 2 in all the cases.

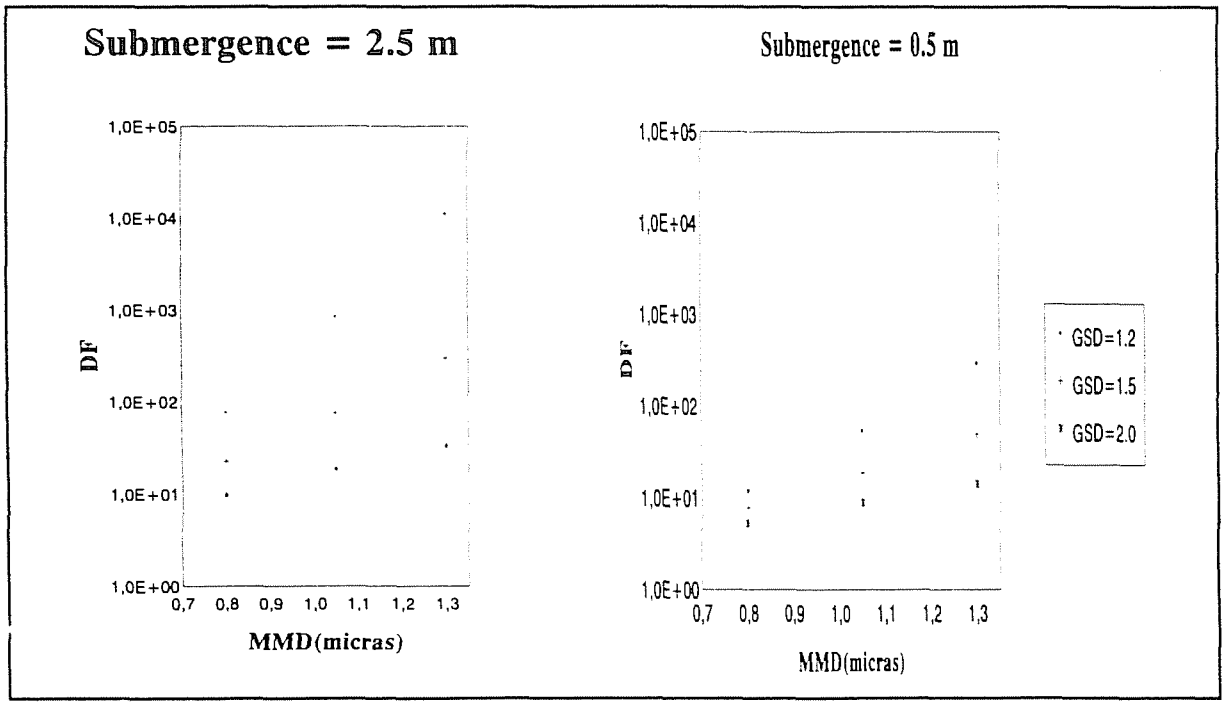

Figure 8. DF uncertainty maps calculated with SPARC vs. size distribution parameters

3.1.3. Hydrodynamic Tests

A total of 10 hydrodynamic tests grouped into two series were carried out. The first series (S1) was characterized by room temperature, whereas the second one (S2) was performed near saturation. Each of this series was in turn splitted into two bins depending on inlet gas composition: without and with steam. As can be realized, inlet gas of b subseries contain steam enough to reach condensing conditions in the pool; S2b subseries injected pure steam. The noncondensible gas used was N_2. Within each subseries inlet gas flow rate was the main variable, ranging from bubble to jet injection regime. Therefore, this test matrix was specifically aimed at studying several influences on hydrodynamics: temperature, gas composition and injection regime. Give the goals pursued in pool scrubbing experiments, the main phenomena to follow were primary bubble formation and its upwards displacement in the region immediately above the injector, where bubble decay takes place. In Table XVI tests specifications are presented.

Table XVI
Hydrodynamic test matrix

			Injection Conditions		Inlet gas		Pool conditions		
Series	Sub-series	Test	T	P	Q	X_s	T	P	S
S1	a	HS1a1	room	1.5	1000.	0.	room	1.	1.5
		HS1a2	room	1.5	2000.	0.	room	1.	1.5
		HS1a3	room	1.5	3000.	0.	room	1.	1.5
	b	HS1b1	120.	1.5	1000.	0.5	room	1.	1.5
		HS1b2	120.	1.5	3000.	0.5	room	1.	1.5
S2	a	HS2a1	120.	1.5	1000.	0.	95.	1.	1.5
		HS2a2	120.	1.5	2000.	0.	95.	1.	1.5
		HS2a3	120.	1.5	3000.	0.	95.	1.	1.5
	b	HS2b1	120.	1.5	1000.	1.	95.	1.	1.5
		HS2b2	120.	1.5	3000.	1.	95.	1.	1.5

3.2. Experimental Results

The experimental results are shown below together with discussions on them. Nonetheless, further interpretation work should be done to maximize benefits from these data exploitation. Specifics on experimental data processing and results discussions can be found in ref. [7].

3.2.1. Pool Scrubbing Tests

The results here presented were obtained from different experimental techniques. Source term into the pool and from the vessel atmosphere was determined by sampling gas flows through filters that were subsequently analyzed by gravimetric techniques and chemical procedures. In addition, samples were taken from the aqueous bulk at the end of the tests. Inlet aerosol characterization was obtained on line by using an optical instrument. The thermohydraulic boundary conditions were satisfactorily controlled during the experiment; namely, target values of these variables were generally met.

Particle size characterization was practically constant during tests RCA1, RCA2 and RCA3. In RCA1, however, the volume distribution measured by the optical device was seen to be rather different from the rest of tests. A large percentage of mass was related to big particle size bins. Experimental evidence showed that it could probably due to large size impurities. RCA2 and RCA3 presented size distributions of a quite similar shape. In Table XVII characteristic parameters of aerosol size distributions are present as a function of time. Table XVIII collects time averages of relevant size distribution parameters.

Table XVII
CMD and GSD of experiments RCA1 and RCA2 and RCA3 along the time

RCA1			RCA2			RCA3		
Time (min)	CMD (μm)	GSD	Time (min)	CMD (μm)	GSD	Time (min)	CMD (μm)	GSD
10.	0.85	1.42	1.	0.90	1.42	8.	0.82	1.37
12.	0.85	1.42	9.	0.89	1.46	10.	0.81	1.36
15.	0.85	1.38	12.	0.86	1.43	13.	0.80	1.37
21.	0.85	1.39	16.	0.85	1.40	18.	0.82	1.39
24.	0.82	1.39	19.	0.85	1.43	21.	0.81	1.38
27.	0.82	1.40	22.	0.86	1.46	25.	0.82	1.40
			25.	0.86	1.46	29.	0.82	1.38
			27.	0.87	1.46			

Table XVIII
Time average properties of size distributions of RCA1 and RCA2 tests

	CMD	GSD	AMMD
RCA1	0.84	1.40	3.52
RCA2	0.87	1.44	3.88
RCA3	0.82	1.38	3.30

During RCA4 test the optical device did not work properly. However, the similar features of aerosol size distributions in the three previous tests suggested that RCA4 distribution should be similar as well. A check of the physical repercussion of those minor differences observed between RCA1 and RCA2 showed that those discrepancies were not relevant for particle absorption in pools.

The aerosol input rates were different in each experiment. As there were two sampling stations at the injection line, a total of four estimations (i.e., gravimetric and chemical analysis) were derived. Despite that different values were obtained, most of them were consistent. Hence, none of them were initially discarded to calculate DFs. Thus, DF ranges appearing below are mostly a consequence of input mass rates discrepancies between the experimental techniques used. Concerning vessel atmosphere sampling, chemical analysis results were seen to be the most reliable, so that filter measurements were not accounted for to derive aerosol outlet mass rates. Experimental DFs were assessed as a quotient between inlet and outlet mass rates of particles:

$$DF = \frac{\dot{m}_{in}}{\dot{m}_{out}}$$

Two sampling stations were located at the vessel atmosphere, one close to the pool surface (TM4) and another at the vessel ceiling (TM3). Hence a total of 8 DFs for each experiment were estimated.In Table XIX DF ranges for each experiment depending on the sampling stations at the atmosphere are shown. As said above, DF ranges represent input mass rates discrepancies from different techniques.

Table XIX
Provisional DF ranges for pool scrubbing tests

	RCA1	RCA2	RCA3	RCA4
TM3	10.6 - 58	75.3 - 190.6	228.5 -392.	2559.5 - 4345.2
TM4	12.4 - 13.2	15. - 40.5	46.6 - 80.	719. - 1220.7

These data are certainly consistent from different points of view: the DF ranges are within the acceptable experimental uncertainty (less than a factor of 3 in all the cases); the same trends were observed in both TM3 and TM4; and, finally, as expected, they indicated that DF increases with submergence.

Nonetheless, an important remark must be done. DFs calculated from TM4 measurements were considered the most reliable ones because of the proximity of this sampling station to the pool surface. Particles escaping from the aqueous volume underwent the effect of several forces along their pathway, being prevented from reaching TM3 sampling station. Given the high density of nickel particles (8.9 g/cm^3), inertial forces and settling were regarded as possible candidates to cause such an effect. Therefore, final estimations of experimental DFs were those of Table XX.

Table XX
Final DFs of pool scrubbing tests

	DF
RCA1	12.4 -13.2
RCA2	16 - 40.5
RCA3	46.6 - 80.
RCA4	719. - 1220.7

3.2.2. Hydrodynamic tests

As said above, attention was drawn to the injection to look at the earlier stages of gas hydrodynamic behaviour: primary bubble formation and detachment, gas movement upwards and gas bulk evolution while rising. The experimental procedure followed was based on image processing recorded with a video camera. Images were taken through four windows placed at two different heights. This equipment arrangement allowed to scan a distance of about 64 cm above injector both laterally and frontally respect to the jet direction.

The primary visual observations appeared to suggest that subseries S1a, S1b and S2a behaved quite similarly, whereas subseries S2b showed a peculiar behaviour. Sub-series S2b featured by a pure steam injection. In these tests a primary bubble formation that suddenly converted mostly into a swarm of very small bubbles (< 1 mm) was observed. This observation must be associated to a fast steam condensation just at the injection point. This, however, was probably due to the extreme conditions imposed (i.e., pure steam injection). It is argued that small noncondensible fraction in inlet gas would change this picture towards much more similar one to the rest of subseries.

Figure 9. Frontal image recorded of the gas structure close to the injector

Concerning gas movement the frontal images showed a marked sequence in gas bulk shape: big gas masses were preceded and followed by very narrow paths linking large globules. However, a regular pattern was not observed in all the tests or along each test. In Figure 9 a digitalized image is shown. Between 32 and 64 cm above the injector big bubbles (around 10-20 cm) were recorded, but small bubbles population increased respecting 0 to 32 cm region. Nevertheless, the fully developed bubbly flow region was not attained.

In Tables XXI and XXII quantitative results of 0-32 cm region and 32-64 cm region, respectively, are presented for S1 series and S2a subseries. A large number of bubbles per experiment was processed (typical figures ranged from 1000 to 2000). Bubble size distributions showed a lognormal shape as bubbles population was represented against bubble volume. The characteristic parameters to describe lognormal distributions were VMD and GSD. The major errors associated to this data analysis came from shortcomings of 2-D image processing and disregard of bubbles smaller than 1 mm.

Table XXI

Size distribution parameters of hydrodynamic tests between 0 and 32 cm from the injector

			Lateral Images		Frontal Images		Total Images	
Series	Sub-series	Test	VMD	GSD	VMD	GSD	VMD	GSD
S1	a	HS1a1	3.84	3.18	3.84	3.16	3.84	3.17
		HS1a2	2.34	2.86	16.08	3.97	9.21	3.40
		HS1a3	1.66	2.65	1.84	2.65	1.75	2.65
	b	HS1b1	7.56	2.96	3.32	2.72	5.44	2.84
		HS1b2	4.19	2.73	1.89	2.40	3.04	2.56
S2	a	HS2a1	2.51	2.51	2.60	2.79	2.78	2.65
		HS2a2	2.03	2.86	2.74	2.68	2.38	2.77
		HS2a3	1.84	2.67	2.61	2.79	2.22	2.73

Table XXI shows that an increase of gas volumetric flow resulted into a decrease in VMD. This observation was seemingly contradictory, but a look into GSD values provides the key for a temptative interpretation. Incoming gas causes an interfacial stress between gas and liquid phases which causes a partial breaking-up of gas main body. The higher the flow, the more efficient the breaking-up. Hence, the VMD decrease is a consequence of the rise of small bubble population at expenses of lowering the amount and the diameter of large bubbles. This interpretation agrees with GSD variation as volumetric flow is increased.

Some exceptions, however, can be seen in the table. Frontal view of HS1a2 test was regarded as anomalous and not considered in this discussion. Frontal images corresponding

to the hot pool conditions did not show any trend as a function of inlet gas volumetric flow rate. Evaporation appears to deaden the effect of the flow and provides similar size distributions in the three cases. However, lateral images confirm that bubble size distribution is affected by flow.

In spite of being consistent with the discussion above, S1b subseries results are quite similar to S1a ones in the frontal image column, but they are more than a factor of two higher in the lateral column. On one side, frontal images are mostly dominated by the view of large bubbles whose large volumes masked partially smaller ones presence due to the shortcomings of 2-D image treatment. On the other, lateral view does not have that constraint along the flow direction and allows to record small bubbles. S1b subseries data could point that under the strong condensing conditions imposed, small bubbles underwent a substantial condensation which made them collapse or reduce their diameter below 1 mm (lower limit imposed to image processing). Thus, bubbles population becomes proportionally richer in larger bubbles and size distribution moves towards higher diameters.

Table XXII

Size distribution parameters of hydrodynamic tests between 32 and 64 cm from the injector

			Lateral Images		Frontal Images		Total Images	
Series	Sub-series	Test	VMD	GSD	VMD	GSD	VMD	GSD
S1	a	HS1a1	1.08	2.33	1.09	2.28	1.08	2.30
		HS1a2	1.19	2.42	1.47	2.30	1.33	2.36
		HS1a3	0.94	2.19	1.44	2.40	1.19	2.30
	b	HS1b1	2.15	2.33	2.62	2.73	2.38	2.47
		HS1b2	1.61	2.11	1.68	2.44	1.64	2.77
S2	a	HS2a1	1.08	2.33	1.27	2.26	1.17	2.29
		HS2a2	1.02	2.25	1.05	2.12	1.03	2.18
		HS2a3	0.91	2.17	0.93	2.08	0.92	2.12

Data in Table XXII show that size distributions moves to lower VMD and GSD values while rising through the pool. Namely, as gas rises-up more smaller bubbles appear at expenses of large bubbles breaking-up so that size distributions moves towards lower diameters and become narrower. Table XXII does not present a noticeable correlation between diameters and the volumetric flow rate; that is, inlet gas regime influence is restricted to the nearby of the injector. However, S1b subseries still presents a smooth effect of the volumetric flow rate. This observation supports the interpretation given above to the difference between lateral and frontal view of this subseries in the 0-32 cm region. As small bubbles disappeared due to sharp condensation, large bubbles dominate the bubble population and still size distribution is centered on bubbles remarkably bigger than in the rest of the cases.

3.3. SPARC and BUSCA Interpretation of Pool Scrubbing Tests

SPARC and BUSCA codes were used to rationalize the retention phenomena occurring in the pool scrubbing tests. All the calculations here presented were performed before getting experimental data necessary to estimate the tests DF, so that they were regarded as blind posttest calculations.

Figure 10 shows DF code predictions together with the experimental DF margins presented in Table XX. Two major observations can be done. On one side, BUSCA largely underestimated DFs in all the cases. The discrepancy was not simply quantitative but qualitative as well. Though DFs of BUSCA tended to increase with submergence, this trend was too weak compared to the experimental one. On the other side, SPARC agreement with experimental data was remarkable. SPARC calculations were bounded by the experimental results. SPARC result of RCA4 was obtained assuming the particle size distribution of RCA2, given that no experimental data were available for this test. SPARC estimate of RCA1 was obtained by adjusting the actual distribution to an ideal lognormal. The experimental volume distribution from the optical device was not considered reliable given the existence of big size particles in this test.

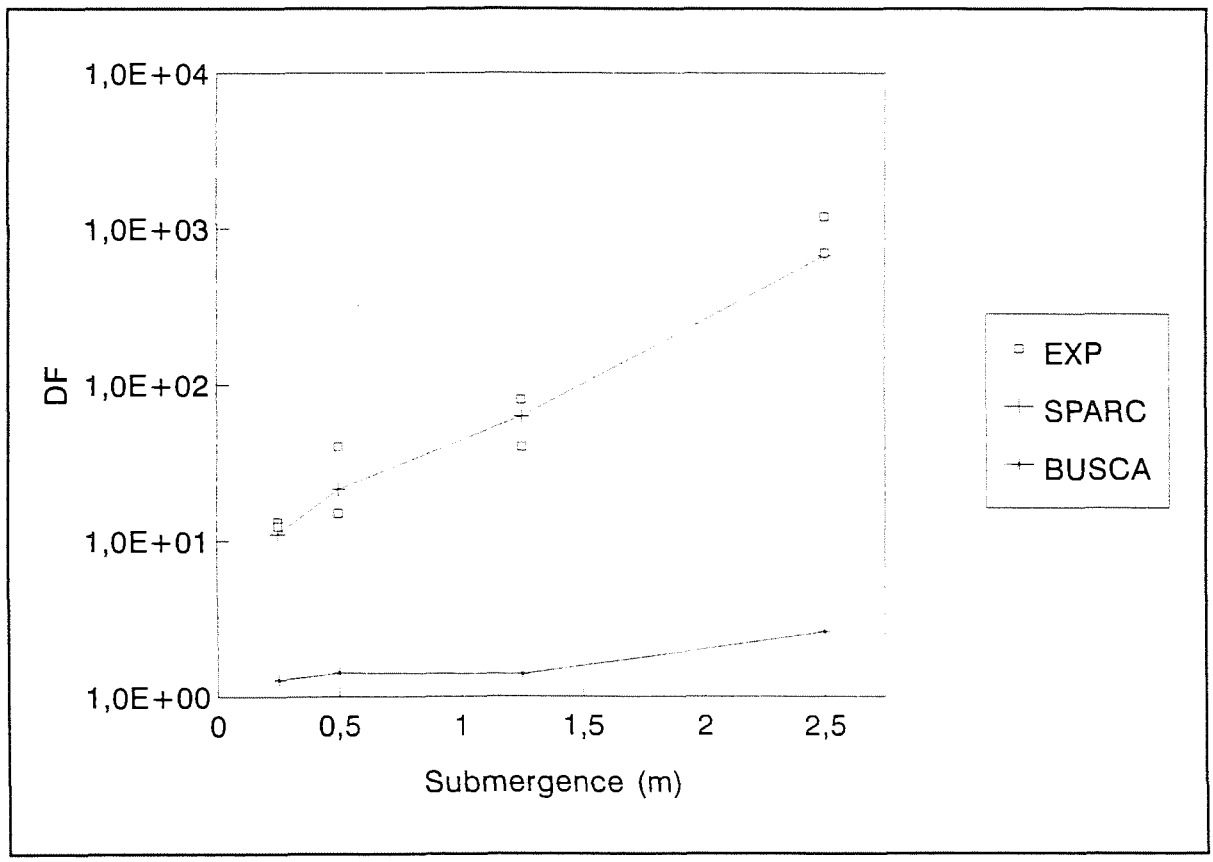

Figure 10. Code - experimental DF comparison

In Table XXIII specific contributions of several phenomena to the total DF are presented for SPARC and BUSCA codes.

Table XXIII
SPARC and BUSCA total and partial DFs for pool scrubbing experiments

	SPARC				BUSCA		
	Injection		Rise-up	Total	Injection	Rise-up	Total
	Impaction	quencher					
RCA1	1.41	6.68	1.17	11.12	1.28	1.00	1.28
RCA2	1.56	7.67	1.79	21.41	1.33	1.07	1.42
RCA3	1.53	5.76	7.10	62.52	1.19	1.17	1.39
RCA4	1.55	7.13	61.45	677.42	1.37	1.91	2.61

SPARC agreement with the experimental data is remarkable. Nonetheless, it should be borne in mind that, in order to enhance the rationalization capability of pool scrubbing scenarios, two important aspects of pool scrubbing were not addressed in this experimental programme: particle growth by steam condensation and particle removal by steam carrying to bubble-pool interface under condensing conditions. The former was prevented by using an unsoluble compound (i.e., metallic Ni). The latter was avoided by considering a steam free carrier gas coming into a close to saturation pool.

In any case, SPARC results fit to these experimental data is unquestionable. As explained in ref. [7], this demonstrates that SPARC global approach to the experimental scenario is suitable: a substantial decontamination of the gas happened just at the injection point in all the cases, while rise-up decontamination grew with submergence. The fraction of the particles retained at the injection point did not show dramatic changes among the tests. SPARC attributes such an early decontamination to the particle absorption occurring during primary bubble formation and detachment. However, this should be confirmed by specific investigation on these mechanisms.

Therefore, under the experimental conditions imposed there are some efficient phenomena removing particles from the bubble near the injector and SPARC succeeded in pointing out it. Further research on this finding would be necessary to validate SPARC formulation of removal mechanisms at the injection and the hypotheses underneath.

4. MAJOR HIGHLIGHTS AND CONCLUSIONS

An extensive research programme on pool scrubbing has been carried out within the Source Term Project of the Third Framework Programme. Several aspects have been addressed: current modelling assessment, new models development and new data acquisition on pool retention and hydrodynamics. Concerning current modelling, the major uncertainties, the most relevant shortcomings and, eventually, the impact of model discrepancies on source term estimates was analyzed based on SPARC90 and BUSCA-AUG92 formulations. Regarding model development a new flow regime of gas rising through the pool was featured and modelled: churn-turbulent regime. Finally, an experimental plan focused on jet injection regime and its associated hydrodynamics was performed and their results discussed and

compared to code predictions. Here below a summary of the major highlights, achievements and conclusions drawn from this work is compiled:

- Low total Decontamination Factors were consistently predicted by both pool scrubbing codes (i.e., BUSCA and SPARC) and PSA codes (i.e., MAAP) during Steam Generator Tube Rupture and Residual Heat Removal bypass sequences.

- Despite that significant discrepancies existed in Decontamination Factors predicted by the two pool scrubbing codes, they were not substantial in terms of Probabilistic Safety Assessment except in the case of the Steam Generator Tube Rupture accident. In this case the higher Decontamination Factors for soluble species calculated by the SPARC code are sufficient to assign the fault to a less onerous release category.

- According to pool scrubbing codes, the injection zone plays a key role in the pool scrubbing scenarios of the above mentioned PWR risk-dominant sequences. Removal mechanisms are closely related to composition and flow rate of the particle carrier gas. In both sequences inlet gas is estimated to come into the pool under jet injection regime. This fact enhances particle deposition by inertial mechanisms. In the case of RHR sequences the inlet gas contains a high steam fraction which turns early condensation into the most important depletion phenomenon.

- Uncertainties in input particle size distribution can largely affect Decontamination Factor estimates for these sequences. On the contrary, submergence uncertainty in the case of the Steam Generator Tube Rupture did not show a remarkable impact on Decontamination Factor calculations.

- Despite its crucial role on pool scrubbing, a scarce database is available on hydrodynamic influence on aerosol retention. Nonetheless, few data seem to point out that particle absorption is enhanced under jet injection regimes and multiorifice injections.

- Based on the current codes hydrodynamic modelling, Decontamination Factor is particularly sensitive to bubble size and swarm rise velocity in the range of interest. Likewise, hydrodynamic phenomenology occurring in the primary bubble decay zone could greatly affect Decontamination Factor of low submergence sequences.

- Hydrodynamic models encapsulated in SPARC and BUSCA are remarkably different in both their basis and their results. In this regard, bubble parameters such as size and shape are particularly relevant given their repercussion on retention mechanisms.

- Present hydrodynamic models show several weaknesses. Particularly important are those related to primary bubble and break-up zone. Initial globule size correlations have not been validated at the high inlet gas flow rates expected in some accident sequences. On the other hand, globule rupture related phenomenology is poorly characterized.

- Some aspects of hydrodynamics are missing in pool scrubbing codes: churn-turbulent flow, pool contaminants and bubble-surface interaction. Churn-Turbulent flow presents hydrodynamic characteristics largely different from that of bubbly regime. Contaminants and, particularly, surfactants can change both bubble boundary conditions and bubble features. Submerged surfaces presence, closely related to accident sequences such as SGTR, can also dramatically change bubble characteristics (i.e., shape and velocity). All these effects currently not accounted for can alter the hydrodynamic boundary conditions and, consequently, the absorption efficiency of the pool.

- A hydrodynamic model to characterize churn-turbulent regime of a gas rising through pools has been developed. The general approach consisting in extending current models to churn-turbulent flow by triggering the application of the churn-tubulent model as certain conditions on superficial gas velocity and mean void fraction are fulfilled. This extension of current models can largely enhance pool scrubbing codes capabilities.

- The different thermohydraulic approach of pool scrubbing codes causes large discrepancies in their particle absorption estimates. The hypothesis of instantaneous thermal equilibrium assumed by SPARC provides a powerful retention mechanism, "early condensation", and allows soluble particles to start to grow as soon as they come into the pool. This last effect makes inertial removal mechanisms more efficient.

- Unlike BUSCA, SPARC accounts the particle removal taking place while globule formation and detachment from the injector. Acting mechanisms (i.e., diffusion, sedimentation and centrifugal deposition), particularly centrifugal deposition, was seen to can remarkably affect Decontamination Factor assessments in some scenarios.

- Particle absorption during bubble rise is a strong function of particle size. Such a function shows a retention minimum usually located between 0.1 and 1.0 μm depending mainly on bubble features. Particles bigger than the size corresponding to the minimum retention are preferentially retained by centrifugal deposition and settling, whereas those smaller are more efficiently removed by diffusion.

  SPARC and BUSCA retention and growth models during bubble rise-up are generally based on the same equations. However, the different approximations taken in each code make predictions show quantitative discrepancies. These divergences become more noticeable in the case of bubble shapes other than spherical one.

- Submicron particles can be effectively retained under specific conditions. On one side, steam condensation on bubble surfaces can carry a fraction of these particles to the pool volume. On the other, as gas comes into the pool at very high flow rates, inertial mechanisms can become efficient even for very small particles. In addition, very small particles are effectively retained by diffusion.

- Pool performance respecting fission product vapours, particularly iodine, could be relevant in terms of both their absorption and their stripping. Depending on conditions along accident scenarios pool could act as either a sink or a source of fission product vapours. This last effect could become especially relevant in scenarios where relatively clean gas bubbles went through a pool with a significant inventory of volatile fission product species.

- Aqueous chemistry is a crucial factor to accurately predict fission product vapour removal from the bubbles. The simple SPARC simulation of inorganic iodine chemistry enables it to follow the experimental trends, whereas BUSCA does not. The capability of estimating long term evolution of pools suggests the convenience of accounting for a more complete chemical scenario, including radiation effects, organics, impurities and so on. This approach points the pool scrubbing-chemistry codes coupling as a suitable way to achieve it.

- Based on previous model assessments, an experimental programme mainly focused on particles retention under jet injection regime was carried out. The major features of this programme were its simplicity (i.e., unsoluble particles, no steam injection, quite a narrow aerosol size distribution) and its representativeness (i.e., near saturate pool, typical particle size, gas injection regime). Submergence effect on retention was studied in four retention experiments. Influences of pool temperature, inlet gas flow rates and composition were looked into by a supporting hydrodynamic programme consisting of 10 tests.

- Experimental Decontamination Factors followed the expected trends with submergence: the larger the submergence the higher the Decontamination Factors. However, it was found that as gas comes into the pool as a jet submergence effect was smoothed from expectations under bubble injection regime. This observation should be confirmed at higher inlet gas flow rates.

- SPARC predictions of Decontamination Factors showed a remarkable agreement with the experimental ones. SPARC calculations pointed that the injection zone contribution was significant and similar in all the tests. As expected, the rise-up decontamination grew with submergence. Unlike SPARC, BUSCA estimates were far away from experimental data, showing less sensitivity than SPARC to submergence and absence of SPARC retention models for small orifices.

- Hydrodynamic tests observations may be explained by assuming that inlet gas flow rates cause a liquid-gas interfacial shear stress at the injection point that partially breaks the gas main body. The higher the flow, the more efficient the breaking-up process. Therefore, small bubbles population rises as inlet gas flow rate was increased. Therefore, besides enhancement of inertial mechanisms under jet injection regime, a significant Decontamination Factor increase should be expected from the transfer surface increase caused by the primary bubble break-up.

- Pool temperature and gas composition did not abruptly affect first stages hydrodynamics, although it was seen that condensation and evaporation processes tended to deaden the effect of interfacial shear stress. In general, similar qualitatively behaviour of gas in the pool was observed in all the tests between 0 and 10 cm. However, above 10 cm those corresponding to pure steam injection showed a remarkable different behaviour. These extreme conditions causes a primary bubble formation that suddenly turns into a swarm of small bubbles. It is argued that small noncondensible fraction in inlet gas would make these case much more similar to the rest.

As an additional result of the work carried out, specific points relevant for source term estimates were found to deserve further research. Here below a short list of major items is presented:

- The experimental plan carried out on jet injection regime should be extended to cover all representative accident conditions. Particularly, it should be done at higher inlet gas flow rates. Up to date, experimental observations and theoretical predictions suggest that dramatic differences compared to bubble injection regime are to be found. Therefore, existing hydrodynamic models should be validated and improved under these conditions and/or new ones could be developed if needed. On the other side, the importance gotten by inertial mechanisms at the injection point in these scenarios suggests that attention should be drawn as well to their check and verification.

- Further development of the churn-turbulent model approach requires single effect hydrodynamic data as well as fission product retention experiments. Verification and validation of current model should be performed to ensure its calculation capability of both hydrodynamics and particle retention.

- Given its potential importance on risk-dominant scenarios the so called "wall effect" should be experimentally studied. The development and implementation in pool scrubbing codes of a model on this issue would give more reliability to code estimates for scenarios such as Steam Generator Tube Rupture accident.

- SPARC assumption of instantaneous thermal equilibrium should be verified and validated. In particular, it should be checked under the specific conditions of Steam Generator Tube Rupture in which it turns into the most significant contribution to Decontamination Factor.

- Pool performance as a source of vapours during late accident stages should be addressed experimentally. Current models cannot predict such a situation, so that this possible additional contribution to source term would be presently ignored. By experimenting it could be weighted how relevant this effect is and models capabilities could be extended and validated.

Finally, a remark should be done concerning actual accident scenarios. A substantial amount of materials will be suspended or dissolved in pool volumes in case of an accident. The capability of these substances to affect pool scrubbing phenomenology should be analyzed